UNIVERSITÀ DEGLI STUDI DI NAPOLI
"FEDERICO II"

UNIVERSITÀ DEGLI STUDI
DI NAPOLI FEDERICO II

Scuola Politecnica e delle Scienze di Base

Area Didattica di Scienze Matematiche Fisiche e Naturali

Dipartimento di Fisica "Ettore Pancini"

Laurea Magistrale in Fisica

Tipologia tesi: Altra tipologia, Osservativa

Gravitational Waves as Cosmological Sirens

Relatori:
Prof.ssa Mariafelicia DE LAURENTIS
Prof.ssa Ester PIEDIPALUMBO
Correlatore:
Prof. Enrico CALLONI

Candidato:
Armando Vittorio RAZZINO
Numero di Matricola: N94000474

Anno Accademico 2018/2019

Contents

Chapter 1

Introduction

The aim to discover as more information as possible about our universe and its components has made researchers aware of the limits of Einstein's General Relativity Theory. In fact it is unable to explain large parts of the evolution of the early universe, as well as other puzzling phenomena of present-day cosmology, such as the absence of magnetic monopoles, the anisotropy and homogeneity of the universe at the last scattering surface and the deviation from expected orbits, topology and dynamics of several objects in the universe. To cope with these issues, starting from the early 1970s, modifications to the current theory and alternative theories of gravity have been proposed, allowing to solve some of General Relativity's problems and to develop further insight on the evolutionary history of our universe and the characteristics of its components.

The challenging part of this process lies not only in the development of a theory itself, but also in understanding what its parameters should be and what their measures should be, in order to justify experimental results and observations. To this end, the search for distance indicators has broadened from standard electro-magnetic sources, like Cepheids, Type Ia Supernovae and Gamma Ray Bursts, towards other interesting objects like coalescing binary systems, the stochastic Cosmic Background Microwave radiation background and also Gravitational Waves sources. The latter are quite relevant, since they represent an independent alternative to electro-magnetic events. This

makes detecting and analysing them a key mean towards the solution of many open conundra in modern-day cosmology and astrophysics. The well known H_0 tension problem, which can be quickly summarized as the difficulty of finding a unique and universal value for the Hubble parameter, that plays a pivotal role in the understanding of the evolution of universe expansion, the investigation of properties of the status equation of Neutron Stars and binary systems, obtaining a better understanding of the early universe and enhancing the capabilities of General Relativity tests at detecting even the smallest deviations from expected orbits, topologies and behaviours are only a few of those riddles to which only partial solutions have been found.

Distance indicators' positions and emitted waves detected frequencies and intensities, just like any other light-speed signal produced within our universe, are influenced by its expansion via the phenomenon known as redshift: light emitted from these objects is reddened and damped in intensity. Therefore, in order to measure their distances one does not only need to know the detected flux over the full wavelength spectrum, the object's nature, geometry, topology and dynamics, but also the relationship between the luminosity distance and redshift and how it is connected to the object's other properties, like its luminosity function and magnitude. This is also valid for gravitational wave sources, but the relationship between luminosity distance and redshift is easier to determine once a proper model for the object hs been developed. This has been done for some objects, among which coalescing binary system during the inspiral phase, that involves the lighter object falling onto the heavier one in a spiral orbit, because of material being absorbed by the latter and its strong gravitational field. The final stage of this phase is a merging of the two objects, which releases a huge amount of energy as well as gravitational and electro-magnetic waves (the latter only manifest with star binary systems, like White Dwarf and Neutron Star ones). The luminosity distance-redshift relationship for the emitted gravitational waves, its connection to the emitted waves intensity and the inspiraling phase dynamics have been well modelled by General Relativity. This allows to study them with ease and exploit their observation in order to solve problems like the H_0 tension and the constraining of alternative theories of gravity's parameters. The first suggestion for these objects to be observed

with some precision, was made by Schutz and others in the 1980s, who dubbed them "standard sirens". They proposed that, if one could observe the same the source with at least three detectors with a signal to noise ratio of at least 30, one could measure the emitted wave intensity and frequency change rate with a 3% uncertainty, allowing to relate it to the luminosity distance-redshift relationship and use this information to invert this relationship and constrain the used theory's parameters, like the cosmographical parameters or the Hubble Parameter. Time has rewarded expectations. In fact, nowadays the advanced Laser Interferometer Gravitational-Wave Observatory (aLIGO) and VIRGO project, with two detectors in the USA (Hanford and Livingston) and one in Italy (Cascina), and the space-based Laser Interferometer Space Antenna (LISA) have allowed to discover several gravitational wave sources and to measure their characteristics. Ground-based interferometers detection have allowed to detect the first Gravitational Wave Sources, granting Thorne, Barish and Weiss the 2017 Nobel Prize in Physics. The discovery of further sources has allowed to create Gravitational Wave sources catalogues like the GWTC catalogue by the aLIGO-VIRGO collaboration and to add candidate sources to existing ones.

The aim of this thesis is to use a catalogue of observed sources, the GLADE catalogue, in order to analyse the propagation of gravitational waves in a modified gravitation theory framework, i.e. an effective Yukawa-like gravitation potential theory, in order to constrain its parameters by assuming that they justify the observed luminosity distance and redshift data. The sources within the GLADE catalogue come from a process of cross-correlation between four different catalogues and include objects like galaxies, globular clusters and galaxy clusters. The main idea behind the work is: if a gravitational wave emitted by an inspiraling binary black hole system (these systems are quite interesting because their coalescence lacks an electro-magnetic counterpart) were to be detected by the aLIGO-VIRGO interferometers, what frequency range should the waves fall into for the modified theory parameters to be within the ranges that have been measured through already performed observations? The candidate sources are linked to already studied ones by comparing them with sources in the GWTC catalogue that lie within the coordinate, luminosity distance and redshift boundaries of selected GLADE sources, in order to understand whether sources from the GLADE

catalogue could actually be candidate Gravitational Wave emissions from inspiraling binary black holes.
The thesis is divided in four chapters:

- **Chapter 2** provides a historical and scientific background behind the search for distance indicators and gravitational wave sources, focusing on what achievements their study would allow to fulfil. The main aim of this chapter is to provide motivations to scour the universe for those objects and to study them.

- **Chapter 3** gives a theoretical outline of the generation and propagation of gravitational waves. This is done first within a generalized framework, then applied to inspiraling binary systems. After that, gravitational wave propagation is first analysed within a General Relativity modelled universe, then within the modified theory, emphasizing the changes the deviation from General Relativity brings to propagation, namely in the luminosity distance-redshift relationship. Finally, the flaws of General Relativity are overviewed, proposing alternative theories as solutions to those and briefly explaining how they solve them.

- Chapter 4 involves the use of the combined GLADE and GWTC catalogues to analyse the parameters of the modified theory, by studying the propagation of gravitational waves that could come from sources within the GLADE catalogue that could be identified with sources in the GWTC catalogue within the error boundaries. Finally, the use of the GLADE catalogue is motivated by an analysis of how it has been created and the benefits of galaxy catalogues in observational cosmology.

- Chapter 5 is a recap of the whole thesis work and contains the conclusions and future perspectives.

Chapter 2

Historical and scientific motivations

This introductory chapter aims to define the main historical and scientific reasons that have lead to the development of a gravitational wave "standard siren" theory. This term, first introduced during the mid-1980s [6], identifies sources which cannot be exploited as distance indicators by using a luminosity function that varies periodically, or at least in a known way, but require a separate theory to study both the signal's propagation from the source to the detector and the signal's generation within the source. Since this thesis' objective is to discuss a standard siren gravitational wave theory, first an outline of the historical and scientific reasons that have brought researchers to develop such a theory shall be given, then various examples of gravitational wave sources shall be described.

2.1 Historical introduction

Around the beginning of the second half of the 1980s, Krolak et al. remarked that a new gravitational wave source had started to become interesting to researchers, adding itself to supernovae and stochastic background, which were then thought to be the

only relevant sources. These sources were coalescing binary systems, especially neutron star and black hole ones [7]. Schutz [6] was one of the first to show how one could use interferometer gravitational wave detectors in order to calculate an estimate value of the Hubble parameter. Using a broadband detector, such as the LIGO detectors (Laser Interferometer Gravitational Observatory) now operating around the world, one can measure both wave frequency and amplitude, as well as additional Post-Newtonian effects. Frequencies include orbital terms as well as multi-pole terms, while amplitude can be calculated as a root mean square, averaged over the detector and source orientation, which both influence the response of the former. Binary systems coalescence events do have an issue: the coalescence rate per year. It depends on the binary system type, it is based on the system components' birth rate and the average binary system "life expectancy" from the outermost stable orbit until coalescence (around 10^8 years). These figures also depend on how the detectors are spread around the world and on the signal-to-noise ratio (S/N): in 1986 Thorne et al. showed that if, for example one considers 4 detectors that identify a source with $S/N = 4 \left(\frac{d_L}{100\ \text{Mpc}}\right)^{-1} \left(\frac{\mu}{1\ M_\odot}\right)^{1/2} \left(\frac{M}{1\ M_\odot}\right)^{1/3} \left(\frac{2f_O}{100\ \text{Hz}}\right)^{-7/6}$, (where d_L is the luminosity distance, μ the reduced mass for the 2-body system, $M_\odot$ is the mass of the Sun, $2 \cdot 10^{30}$ kg, M is the total mass and f_O the orbital frequency) each, all at the same time, they would be able to detect 1 neutron star binary system coalescence within 800 Mpc every year and 1 black hole system (around 10 $M_{/odot}$) coalescence within 4 Gpc every year [8].

In the same article by Krolak et al., the authors suggested that one could use gravitational waves from sources within 100 Mpc in order to measure the luminosity distance with an error of a few percent. Sadly, those events are in general not (except neutron star systems coalescences) accompanied by an electromagnetic wave event counterpart, therefore it is quite difficult to obtain the source's redshift with enough precision to measure the Hubble constant with an error of a few percent (the method to perform this calculation is described in chapter 3).

They also suggested their use as distance indicators, if one could be able to determine

the source's host galaxy. This task is unfortunately often made quite arduous by the generally irregular galaxy distribution within the luminosity distance "error volume", therefore one should perform a statistical analysis within this distribution and find what galaxies could be the most probable host candidates (a quite recent study of this kind, that also includes an application to the determination of the Hubble Parameter can be found in [54]).
The article eventually suggested additional measurements that could be performed by analysing gravitational waves from binary system coalescences with LIGO detectors, such as measuring mass distributions in non-cosmologically large zones (around 500 - 600 Mpc) of the universe, polarization and propagation tests for gravitational waves, measurements of the mass density of the universe and study of the history of stellar formation. Alas, these topics are beyond the scope of this thesis, therefore they won't be analysed further here.

Time has eventually allowed to pursue those objectives, and others as well. In fact, the latest 2 decades have seen the development and rise of LIGO detectors and their use has allowed researchers to discover the first gravitational wave event, namely the discovery of source GW170817, that has allowed the aLIGO-VIRGO collaboration. more specifically Weiss, Barish and Thorne, to obtain the Physics Nobel Prize in 2017 [49]. Nowadays, there are 3 active LIGO detectors, namely the aLIGO-VIRGO collaboration with detectors located in Hanford, (Washington, United States of America), Livingston (Louisiana, United States of America) and Cascina (PI) (Toscana, Italy) [41] and they have allowed to observe several transient Gravitational Wave sources, covering an area of hundreds of square degrees, also considering signal to noise ratios and source locations with respect to the detectors [42] [47]. Furthermore, they have allowed researchers to perform follow-up observations (such as the work described in [44]).

The main Gravitational Wave observation objective, as far as this thesis is concerned, that will be further discussed in section 2.2, is the search for a solution to the problem known as the H_0 tension through the discovery of new distance indicators. This issue

shall now be briefly discussed.

The Friedmann-Robertson-Walker-Lemaitre cosmological model, also known as the Standard Cosmological model, is the starting point of all gravitational theories based on Einstein's Theory of General Relativity and it is used as the model for the description of Gravitational Wave propagation in section 3.4.1. This model describes our universe as a system that is undergoing a process of expansion: a key parameter in this model is the so-called "scale factor" $a(t)$. This parameter allows to understand how the expansion of the universe has changed through time and is directly correlated to the cosmographical Hubble parameter $H(t_0)$, defined as

$$H_0 \equiv H(t_0) = \left(\frac{da}{dt}\right)_{t=t_0} \frac{1}{a(t_0)} \tag{2.1}$$

The Hubble parameter measures the speed of the universe expansion rate at time t_0 from the first light-matter separation event, therefore its value retains a paramount importance towards the understanding of the universe at any given time. The Hubble parameter's relationship with gravitational redshift is the main method for its value to be measured: this means that H_0 can be measured by observing a wave signal from a source in the observable universe at a given time. The wave signals that have been used are Electro-Magnetic and Gravitational Waves, allowing to obtain independent H_0 measurements. The Planck mission observations [39] have allowed to obtain a first H_0 value of $H_0 = (67.8 \pm 0.9)$ km s^{-1} Mpc^{-1} by observing temperature and polarization anisotropies in the Cosmic Background Microwave radiation, assuming a Λ Cold Dark Matter FRWL cosmological model. The use of several different Electro-Magnetic wave sources has allowed as many other measurements [43], all of which are consistent within either 2σ or 3σ with the Planck collaboration measurement. Some of these are the "H0LiCOW" project [51] measurement , which has given $H_0 = (71.9 \pm 2.7)$ km s^{-1} Mpc^{-1} through the observation of quasars and the use of time-delay cosmography, the measurement made by Riess et al. [46] through the observation of Type Ia Supernovae and a measurement of galaxy NGC4258 distance from maser data, which has given $H_0 = (73.24 \pm 1.74)$ km s^{-1} Mpc^{-1}.

A gravitational wave measurement is made very difficult by the challenge represented

by understanding from what specific area of the universe the signal comes from, i.e. what galaxy is the closest to the source: the galaxy density in the area can be high, since luminosity distance errors from gravitational wave measurements tend to be very large [55] (they can go beyond 50% of the measured value). An effort has been made by aLIGO-VIRGO collaboration to do something of the sort [53], but the methods described within go beyond the scope of this thesis. Therefore, the value of H_0 will be assumed as equal to the one observed by the Planck collaboration. Figure 2.1 shows a comparison of some of these measurements and their uncertainties.

Since each measurement comes from a different source, this creates confusion about what value to use for a precise description of the situation of the universe expansion at the present day. The answer to this conundrum is still unknown, therefore the choice one makes has to be evaluated time by time, accurately choosing which H_0 value is the most suitable for the application.

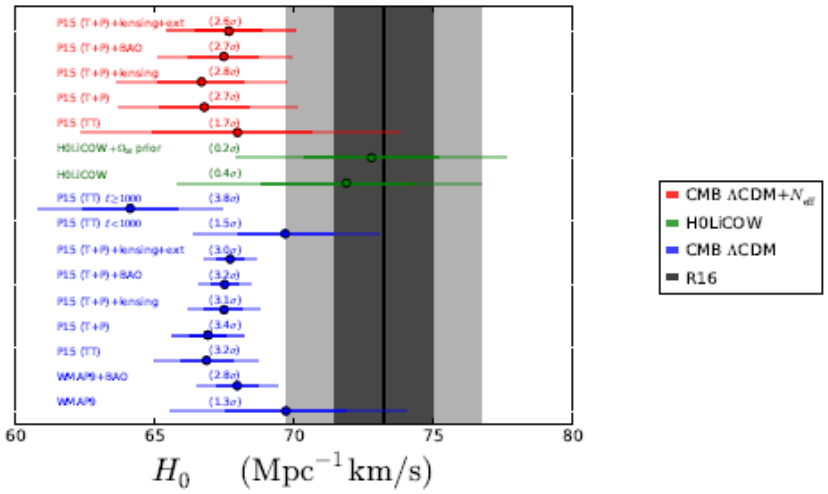

Figure 2.1: Measurements of H_0 from several different projects. It can be clearly seen how much they differ in uncertainty and how those uncertainties overlap within 2σ and 3σ discrepancies. In parenthesis, the discrepancy with the Planck measurement is indicated.

Because of what has been said above, it can be clearly seen why nowadays gravitational

waves are a phenomenon of great importance and what objectives their study allows to achieve. Now a more in-depth discussion of the concepts of distance indicators, standard candles and standard sirens shall be given.

2.2 Distance indicators and standard sirens

This section intends to give a general description of the most important types of distance indicators currently used in Astrophysics. This is done in order to add a more solid motivation to the use of electro-magnetic and gravitational waves to study the evolutionary history of the universe.

Since the positions of objects in our universe are subject to change not only because of their proper motions, but also because of the universe expansion process, the use of redshift and luminosity distance (see chapter 3.5 for definitions of these concepts) is necessary in order to give a proper measurement of their distances and position. Moreover, since an object's redshift can be used in order to calculate its age, this can give crucial information about the universe evolution and history.

Now a summary of the main distance indicators, also known as standard candles, shall be given. The term "standard candle" refers to an object whose luminosity function with respect to time is known. This function can be a periodic one (e.g. Cepheid variables) or a somewhat peaked one (e.g. Supernovae and Gamma Ray Bursts) and it plays a pivotal role in the determination of the object's luminosity distance.

- Stars and galaxies are the easiest standard candles that can be observed. They have been used for this kind of purpose since the 1970s [4] and include several different types of objects. *Cepheid variables* are very bright population I, i.e. they are rich in heavy elements due to their relatively recent formation, stars [19] whose stability, wide availability and easy physical understanding allow for them to be very convenient objects of study. Thanks to the Hubble Space Telescope, researchers have been able to locate Cepheids farther than 30 Mpc.

Very similar to Cepheids in their standard candle character are *RR Lyrae*. They act as calibrators for extragalactic globular clusters distance measurements and serve as standard candles within distances closer than the Magellanic Clouds. *Spectral Type A and B Supergiants*, thanks to the work of Chalonge and Divan [2] who have measured their luminosity functions' parameters and their errors, can also be used as standard candles. *White Dwarf binary systems* also serve as standard candles. In fact, "nova events", i.e. the phase of a binary system's life cycle when the the primary star (the one whose mass is the largest) enters a state of instability caused by an excessive enlargement due to its mass having been increased through the absorption of gas from its partner, and then releases this mass through an explosion [48], can be used as standard candles, because the relationship between the magnitude and the decay rate parameter is known to be in the form $M = a + b\log(t_3)$ where t_3 is the decay parameter and a and b are constant terms that can be obtained through mean square fitting. This method has been developed by D. B. McLaughlin [1].

- *Type Ia Supernovae* are events similar to novae, but they happen in binary systems when the nova event is triggered by a star whose mass exceeds the Chandrasekhar limit of $1.4M_{\odot}$, causing a Supernova explosion that is one of the possible fates of a White Dwarf binary system [48]. The use of these objects as standard candles [12] has been introduced by Wheeler and Harkness [11], who determined their light curves through the observation of the decay of radioactive Nickel ejected by the explosion. Works such as the ones by Hamuy et al. [14], Tamman and Leibungdut [10] and Capaccioli et al. [9] have allowed to measure absolute magnitude scatters up to 0.3 mag. The uses of Type Ia Supernovae in cosmology are various. One can use them to study peculiar velocities and motions of neighbouring objects [13] and measure the value of the Hubble parameter by using a relationship between it and B band magnitude:

$$M_B = \mathscr{A} + 5\log\left(\frac{H_0}{100\text{ km s}^{-1}\text{ Mpc}^{-1}}\right) \tag{2.2}$$

where $\mathscr{A}$ is a constant depending on what object is observed.

Another test that Type Ia Supernovae allow to perform is the time dilation test for the expansion of the universe. This test involves the determination of delays within the light curves of Type Ia Supernovae whose redshift is known [3]. Finally, some studies have been made in order to measure magnitude changes for Type Ia supernovae whose redshift is known, by setting a value of the deceleration parameter q_0 (see chapter 3.4.1 for a description of it), allowing to give an estimate of this parameter [5].

- *Gamma Ray Burst* events are thought to be generated by Supernova explosions of single stars (Long Soft Gamma Ray Bursts) or by coalescences of binary systems containing white dwarfs (Short Hard Gamma Ray Bursts). They possess high energy and brightness, allowing for them to outshine the host galaxy and to be easily observed. Gamma Ray Bursts can be used to measure relative density cosmological parameters [33], that are defined as

$$\Omega_c = \frac{\rho_c}{\rho_{\text{crit}}} \tag{2.3}$$

where ρ_c is the cosmological density of a component of a cosmological universe model (matter, radiation, cosmological constant, scalar field etc.) and ρ_{crit} is the universe critical cosmological density, defined as

$$\rho_{\text{crit}} = \frac{3\,(H_0)^2}{8\pi G} = 8.5 \cdot 10^{-23}\ \text{kg m}^{-3} \tag{2.4}$$

where $H_0 = 68$ km s^{-1} Mpc^{-1} and G is the universal constant of gravitation.
Gamma Ray Bursts have been observed up to redshift $z = 6.29$ [29], therefore they can be used to explore areas of the early universe other sources don't allow to discover. They can be used to study the properties of matter observed in absorption and extinction along the line of sight [31], to probe the initial mass function of the stars whose explosion they come from [32], to study the characteristics of the Inter-Galactic Medium through spectroscopic studies [27] and to pose constraints on the universe dark matter density and content, in terms of a dark matter relative cosmological density Ω_{dm} defined as in equation (2.3), and

also on the density of the cosmological constant component Ω_Λ [30]. The cosmological constant is an artefact: there exist several models for it and they all aim to introduce a component able to "drive" the universe expansion. This allows to go beyond the limits of Einstein's General Relativity theory, which does not allow for an accelerating expansion of the universe, that is instead proposed by various models like the Λ Cold Dark Matter model and the scalar field model. A more detailed description of these theories goes beyond the purposes of this thesis and can be found in works such as [36] and [50].

- *Supermassive Black Holes* accretion processes, especially the ones within the centre of galaxies (Active Galactic Nuclei or AGN), represent a very interesting phenomenon [40] since they can be studied at redshifts up to $z = 7$, allowing a deeper understanding of the universe at large distances [37] and of the early universe. AGN are characterized by a known relationship between their luminosity and their mass. Such a relationship takes into account the AGN's mass accretion rate, redshift, observed radiation wavelength, accretion disk model and energy dissipation. The obtained formula is

$$\dot{M}_{\rm bh}\,(d_L) = 0.53 \left(\frac{\frac{4\pi (d_L)^2 \lambda (1+z) F_\lambda}{10^{44}\ \mathrm{erg\ s^{-1}}}}{\cos i} \right)^{3/2} \left(\frac{M_{\rm bh}}{10^7\ \mathrm{M_\odot}} \right)^{-1} \mathrm{M_\odot\ yrs^{-1}} \tag{2.5}$$

  where $\dot{M}_{\rm bh}$ is the mass accretion rate expressed as a derivative of the mass with respect to time, F_λ is the observed flux at $\lambda = 5100$ Å and i is the angle of inclination of the accretion disk with respect to the line of sight. Therefore,if one knows the Black Hole's mass, redshift and flux, one can measure its luminosity distance, by assuming an averaged value for $\cos i$, based on what AGN type one is considering.

- *Gravitational waves* can also serve as distance indicators [28], as already anticipated at the start of this chapter. Chapter 3 gives a physical and mathematical explanation of how to do so. Therefore, this section will only briefly introduce this topic. The coalescence which happens at the end of the inspiraling process

of binary systems, which shall be explained further in 2.3, is one of the primary sources for gravitational waves. The early inspiral phase of binary systems has been well modelled and therefore gravitational waves generation from those systems can be easily linked to their redshift and luminosity distance. The main challenge lies in precisely locating the system. As suggested by Schutz (see the above reference), this could be done if the coalescence produced an Electro-Magnetic counterpart to the Gravitational Wave emission. This only happens in star binary systems, therefore one cannot always use these types of objects as distance indicators. The error in the luminosity distance is also caused by the system's magnification and de-magnification because of gravitational lensing effects. These and other factors make the use of Gravitational Waves sources as distance indicators as challenging as it is interesting. The latest advancements in the observation of these objects has allowed to shed some light over them and they still remain a very promising alternative to Electro-Magnetic sources towards the goal of adding an independent measurement to the H_0 tension problem.

As it can be seen from the above description, our current observation capabilities allow to explore a wide variety of distance indicators. This gives this kind of objects a great value in terms of probes for the discovery of the properties of matter in our universe and the study of its history and evolution.

Since this thesis is mainly centred around Gravitational Waves, the following section will describe what kind of objects produce such waves in our universe.

2.3 Gravitational wave sources

Through the use of both ground based and space-based, like the LISA project, interferometers, it has been possible to detect gravitational waves from several different sources. The easiest way to differentiate these sources is via the frequency of the detected waves [25]. Therefore, detected waves can be divided in:

- *Extremely Low Frequency* waves have frequencies in the 10^{-18} Hz - 10^{-15} Hz range. The only way these waves can be sought is via their imprint on the Cosmic Background Microwave Radiation (CMB) [24]. This ensemble of sources is also known as the stochastic background. In order to perform an analysis of these sources, one needs to use at least 2 independent detectors, since such a low frequency can easily overlap with the detector noise. The stochastic background can be used to understand the characteristics of the very early universe, since this stochastic background is thought to be from that period. These very early universe waves, which superstring theories models predict to be after 10^{-25} s after the Big Bang, could have been subject to a redshift that may have brought them in the LIGO detectors range, allowing us to observe them. Vibrations in strings created in the very early universe could have produced the stochastic background we nowadays observe [20]. It could also have been produced by occasional and individual vibration spikes in the strings, created by connection points (or kinks)between the strings themselves [22]. For this reason, the stochastic background can be a useful tool towards the study of experimental proofs of string theory models.

- *Very Low Frequency* waves have frequencies in the 10^{-7} Hz - 10^{-9} Hz range. These waves are sought through pulsar timing [26] and are thought to be produced by extremely massive (i.e. having a mass much larger than 10 $M_{\odot}$) Black Hole binary systems in the early universe. Gravitational waves from these sources ae likely to be produced during the ring-down final phase of the coalescence. During this phase, the Black Hole created by the merging slowly pulsates towards its stabilization, after a very violent space-time geometry distorting merger phase [17]. Merger and ring-down phases waves dominate the Gravitational Wave spectrum of the source when the components mass exceeds 200 $M_{\odot}$. It is thought that such massive objects could have formed in dense star clusters, allowing waves of this kind to be used as probes for these kinds of environments.

- Low frequency and *High Frequency* waves cover the 10^{-4} Hz - 1 Hz range and the 1 Hz - 10^{4} Hz range respectively. They belong to space Gravitational Wave

Interferometer LISA's and the aLIGO-VIRGO collaboration ground-based detectors detection ranges respectively. This category includes the highest variety of sources. Inspiraling Neutron Star, White Dwarf and Black Hole binary systems, of which the latter are the ones this thesis' work is interested in, are well known and modelled objects. The inspiraling phase starts when the system reaches gravitational stability and happens because of matter flowing from the lighter component towards the heavier one, causing the former to slowly inspiral towards the latter as they describe a mutual quasi-circular orbit. The combined use of space-based and ground-based detectors allows for sources of redshift up to $z \sim 2$ to be discovered in this category, making them alternative tools for the study of the recent and present-day universe. Kalogera et al. [23] have calculated very encouraging event rates of between 1 and 800 per year for Neutron Star system coalescences, between 1 and 1500 per year for hybrid systems containing one object per type and between 30 and 4000 per year for Black Hole system coalescences. For this reason, these kinds of sources have a quite large availability, allowing for even tens of thousands of sources to be potentially discoverable within a single year of observation.

Hybrid Black Hole-Neutron Star systems involve the star to be tidally disrupted and distorted by the proximity to its companion and its very intense gravitational field. Waves produced during the inspiral phase of these systems could carry information about the Neutron Star equation of state, for example allowing to measure the star's radius with a 15% uncertainty for sources within 140 Mpc [21].

Within the low and high frequency waves category also lie the ones produced by Type II Supernova explosions, i.e. the ones that happen when a stellar core collapses into a Neutron Star or Black Hole. Gravitational Waves from these sources could allow the determination of the core's non-spherical dynamics during the last milliseconds before the explosion, allowing to predict the object's final stage as either a Neutron Star or Black Hole respectively. An event rate of 1 every 30 years for this kind of events has been measured within the Magellanic Clouds [15].

Cosmic Gamma Ray Bursts also belong to this category. They are observed at least once a day by space-based detectors and are thought to be originated by either the coalescence of binary systems that cause the final object to be a Black Hole, or by relativistically heated rapid inflows of gas on newborn Black Holes. The strong Gravitational Waves Cosmic Gamma Ray Bursts generate, carry information about their source's nature. It is expected that up to 2 events per year as far as 1.55 Gpc could be detected through the use of Gravitational Waves interferometers.

Finally, low frequency waves can allow the study of very fast rotation dynamics in newborn Neutron Stars. This rotation, that not always includes a conservation of the total angular momentum, allows for the outermost layer of the star to crystallize and its shape to change from a very eccentric elliptic form to a more circular one. The emission of Gravitational Waves concurs with electro-magnetic torques associated with the star's spinning magnetic field and pulsar emission. The emission of these waves can be also correlated with the star's temperature stabilization within the 10^9 K - 10^{10} K range [16].

This long and wide list of sources and possible applications make Gravitational Waves a core phenomenon to study if one wants to obtain more information concerning the properties of our universe throughout the whole of its history. Their analysis has and will surely shed some light on many unanswered conundra of modern-day astrophysical and cosmological research.

As anticipated above, this thesis will be concerned with Gravitational Waves produced by Black Hole binary systems during the inspiral phase of their evolution. This is because modelling this phase is much easier than the merger and ring-down phases and can be easily done within the General Relativity Standard Cosmological theory. A more thorough analysis of this model will be given in the next chapter.

Chapter 3

Theoretical analysis

The aim of this first chapter is to obtain luminosity distance as a function of redshift, using gravitational waves emitted by coalescing binary systems, within a general relativity framework. This shall be done from a theoretical point of view. Firstly, the gravitational wave tensor field equations shall be derived from a non-linearized theory, then this theory will be applied to gravitational waves emitted by a binary system. Finally, the chapter will examine gravitational wave propagation within a Friedmann-Robertson-Walker-Lemaitre cosmological model, in order to understand what happens to gravitational waves as they travel from the source to the observer.

3.1 Gravitational Waves in General Relativity from a linearized theory

To begin with, the general form for a gravitational wave has to be derived from a geometrical approach: this will be done following the steps outlined in [34]. The starting point is the gravitational action:

$$\mathscr{S} = \mathscr{S}_E + \mathscr{S}_M = \frac{c^3}{16\pi G}\int d^4x\sqrt{-g}\,(R + l_M) \tag{3.1}$$

where $\mathscr{S}_E$ is the Einstein action component and $\mathscr{S}_M$ is the matter component with l_M as the matter lagrangian density, c is the speed of light in a vacuum, G is the universal gravitation constant, g is the metric determinant and $d^4x = cdtd^3x$, with the coordinate convention $x^\mu = \left(cdt = x^0, x^1, x^2, x^3\right)$. The action shall be varied with respect to a metric transformation $g_{\mu\nu} \to g_{\mu\nu} + \delta g_{\mu\nu}$. R is the Ricci scalar, obtained from the Ricci tensor $R_{\mu\nu}$ through $R = g^{\mu\nu}R_{\mu\nu}$. The Ricci tensor is $R_{\mu\nu} = R^\alpha_{\mu\alpha\nu}$ (the Einstein convention of a sum over repeated indexes is used), with the Riemann tensor defined as $R^\mu_{\nu\rho\sigma} = \partial_\rho\Gamma^\mu_{\nu\sigma} - \partial_\sigma\Gamma^\mu_{\nu\rho} + \Gamma^\mu_{\alpha\rho}\Gamma^\alpha_{\nu\sigma} - \Gamma^\mu_{\alpha\sigma}\Gamma^\alpha_{\nu\rho}$ and the Christoffel symbols are related to the metric thanks to the relation $\Gamma^\rho_{\mu\nu} = \frac{1}{2}g^{\rho\sigma}\left(\partial_\mu g_{\sigma\nu} + \partial_\nu g_{\sigma\mu} - \partial_\sigma g_{\mu\nu}\right)$. The variation of $\mathscr{S}_M$ yields:

$$\delta\mathscr{S}_M = \frac{1}{2c}\int d^4x\sqrt{-g}T^{\mu\nu}\delta g_{\mu\nu} \tag{3.2}$$

where $T_{\mu\nu}$ is the matter energy-momentum tensor. By varying the full action, one obtains the well-known Einstein equation:

$$R_{\mu\nu} - \frac{1}{2}g_{\mu\nu}R = \frac{8\pi G}{c^4}T_{\mu\nu} \tag{3.3}$$

The approach to the quest for a solution to this equation (i.e finding the unknown metric $g_{\mu\nu}$) shall be done through the use of a *linearized theory*. Such a theory involves the solution taking a form:

$$g_{\mu\nu} = \eta_{\mu\nu} + h_{\mu\nu} \tag{3.4}$$

where $\eta_{\mu\nu}$ is the Minkowskian flat space metric, represented as $\eta_{\mu\nu} = \text{diag}\,(-1,1,1,1)$, and $h_{\mu\nu}$ is a symmetrical tensor which represents an "infinitesimal" deviation from the flat metric with the condition $|h_{\mu\nu}| \ll 1 \;\forall\; \mu,\nu$. The linearized theory's aim is to expand the Einstein equation to linear order in $h_{\mu\nu}$. General relativity invariance with respect to continuous, differentiable and invertible, with a differentiable inverse, coordinate transformations of the form $x'^\mu = x^\mu + \xi^\mu(x)$, shall be assumed. Through such transformations the metric transforms itself as:

$$g'_{\mu\nu}(x') = \frac{\partial x^\rho}{\partial x'^\mu}\frac{\partial x^\sigma}{\partial x'^\nu}g_{\rho\sigma}(x) \tag{3.5}$$

and $h_{\mu\nu}$ transforms as:

$$h'_{\mu\nu}(x') = h_{\mu\nu}(x) - \left(\partial_\mu \xi_\nu + \partial_\nu \xi_\mu\right) \tag{3.6}$$

where $|\partial_\mu \xi_\nu|$ is of the same order of smallness as $|h_{\mu\nu}|$ and terms of second order and higher have been neglected . These conditions ensure the invariance of linearized theory under transformations of this kind. This invariance is not the only one that could be assumed: e.g. one could assume invariance under Poincarè transformations of the nature $\Lambda^\mu_\nu + a^\mu$ where the boost components of the Lorentz transformations Λ^μ_ν have to be chosen as ones that keep the $|h_{\mu\nu}| \ll 1$ condition.
To linear order in $h_{\mu\nu}$, the Riemann tensor is:

$$R_{\mu\nu\rho\sigma} = \frac{1}{2}\left(\partial_\nu\partial_\rho h_{\mu\sigma} + \partial_\mu\partial_\sigma h_{\nu\rho} - \partial_\mu\partial_\rho h_{\nu\sigma} - \partial_\nu\partial_\sigma h_{\mu\rho}\right) \tag{3.7}$$

In order to write a more compact form for the Einstein equation in linearized theory, some definitions shall be given:

$$h = \eta^{\mu\nu} h_{\mu\nu} \ , \ \bar{h}_{\mu\nu} = h_{\mu\nu} - \frac{1}{2}\eta_{\mu\nu} h \tag{3.8}$$

The Einstein equation in linearized theory takes the form:

$$\Box \bar{h}_{\mu\nu} + \eta_{\mu\nu}\partial^\rho\partial^\sigma \bar{h}_{\rho\sigma} - \partial^\rho\partial_\nu \bar{h}_{\mu\rho} - \partial^\rho\partial_\mu \bar{h}_{\nu\rho} = -\frac{16\pi G}{c^4} T_{\mu\nu} \tag{3.9}$$

where $\Box = \eta_{\mu\nu}\partial^\mu\partial^\nu$ is the flat-space Dalembertian operator. A gauge choice will be used in order to simplify the equation: the De Donder gauge

$$\partial^\nu \bar{h}_{\mu\nu} = 0 \tag{3.10}$$

implies that the transformation for $h_{\mu\nu}$ introduced in (3.6) becomes, in terms of $\bar{h}_{\mu\nu}$:

$$\bar{h}'_{\mu\nu} = \bar{h}_{\mu\nu} - \left(\partial_\mu \xi_\nu + \partial_\nu \xi_\mu - \eta_{\mu\nu}\partial_\rho \xi^\rho\right) \tag{3.11}$$

The resulting transformation for the De Donder gauge is:

$$\left(\partial^{\nu}\bar{h}_{\mu\nu}\right)' = \partial^{\nu}\bar{h}_{\mu\nu} - \Box\xi_{\mu} \tag{3.12}$$

Therefore, if one wants to keep the form of the De Donder gauge under this transformation, ξ_{μ} has to solve a residual gauge equation:

$$\Box\xi_{\mu} = f_{\mu}(x) \tag{3.13}$$

where $f_{\mu}(x)$ is some function of x such that $\left[\partial^{\nu}\bar{h}_{\mu\nu}\right]_{t=0} = f_{\mu}(x)$.
Equation (3.13) always admits a solution in the form:

$$\xi_{\mu} = \int d^4x \mathscr{G}(x-y) f_{\mu}(y) \tag{3.14}$$

where the Green function $\mathscr{G}(x)$ has to solve:

$$\Box_x \mathscr{G}(x-y) = \delta^4(x-y) \tag{3.15}$$

where $\delta^4(x-y)$ indicates the four-dimensional Dirac delta distribution. Once the De Donder gauge has been established, the linearized equation takes on the much more simplified form:

$$\Box\bar{h}_{\mu\nu} = -\frac{16\pi G}{c^4} T_{\mu\nu} \tag{3.16}$$

This equation implies that the matter energy-momentum tensor must satisfy a continuity equation $\partial^{\nu}T_{\mu\nu} = 0$.
Linearized theory therefore implies that the gravitational wave sources are objects that move in flat space-time along the geodesics generated by their mutual influence. The use of the flat-space metric underlines that the source's dynamics are described using Newtonian gravity.

In order to study gravitational waves propagation outside the source, one needs to solve

the homogeneous wave equation:

$$\Box \bar{h}_{\mu\nu} = 0 \tag{3.17}$$

A straightforward result is that gravitational waves travel at the speed of light, since $\Box = -\frac{1}{c^2}\partial_t^2 + \nabla^2$. Moreover, outside the source, the De Donder gauge still holds for a transformation of the coordinates in the form $x'^{\mu} = x^{\mu} + \xi\mu$, where ξ_{μ} satisfies the residual gauge $\Box\xi_{\mu} = 0$ and $\Box\xi_{\mu\nu} = 0$, where
$\xi_{\mu\nu} = \partial_{\mu}\xi_{\nu} + \partial_{\nu}\xi_{\mu} - \eta_{\mu\nu}\partial_{\rho}\xi^{\rho}$. This last condition can be used to bring the six independant components of $\bar{h}_{\mu\nu}$ to only two (the De Donder gauge is used to bring the initial 10 independant components of $h_{\mu\nu}$ to 6). This is done by using the arbitrary ξ_{μ} functions to impose four conditions on $\bar{h}_{\mu\nu}$. To begin with, ξ^0 is chosen so that $\bar{h} = \eta^{\mu\nu}\bar{h}_{\mu\nu} = 0$, which implies that $\bar{h}_{\mu\nu} = h_{\mu\nu}$. Then, the other 3 functions ξ^i are chosen such that $h^{0i} = 0$. Therefore, the De Donder gauge with $\mu = 0$, that is $\partial^0 h_{00} + \partial^i h_{0i} = 0$, becomes $\partial^0 h_{00} = 0$. Phisically, this represents the Newtonian potential of the source, which is therefore time-independant: the gravitational wave is the time-dependant part, so $\partial^0 h_{00} = 0$ implies that $h_{00} = 0$. Thus, one has $h_{\mu 0} = 0 = h_{0\mu}$. One can fix conditions on the spatial part h_{ij} through the spatial part of the De Donder gauge $\partial^j h_{ij} = 0$. Therefore, the conditions imposed on $h_{\mu\nu}$ are:

$$h_{0\mu} = 0 = h_{\mu 0},\ h_i^i = 0,\ \partial^j h_{ij} = 0 \tag{3.18}$$

where h_i^i is the trace of $h_{\mu\nu}$. These 3 conditions define the *transverse traceless gauge*, in which the metric deviation shall be denoted as h_{ij}^{TT}.
The homogeneous wave equation has an elementar plane wave solution $h_{ij}^{TT}(x) = \varepsilon_{ij}(\vec{k})e^{ikx}$, where $\varepsilon_{ij}(\vec{k})$ is the polarization tensor and k is the wave vector $k^{\mu} = (\frac{\omega}{c}, \vec{k})$, with $|\vec{k}| = \frac{\omega}{c}$ and $kx = k_{\mu}x^{\mu}$. Introducing the propagation direction $\hat{n} = \frac{\vec{k}}{|\vec{k}|}$ and choosing

it along the $x^3 = z$ axis, the polarization tensor takes the form:

$$\varepsilon_{ij}(\vec{k}) = \begin{pmatrix} h_+ & h_\times & 0 \\ h_\times & -h_+ & 0 \\ 0 & 0 & 0 \end{pmatrix} \tag{3.19}$$

Therefore, using the convention of taking only the real part of the solution h_{ij}^{TT}, one obtains the result:

$$h_{ij}^{TT}(t,z) = \begin{pmatrix} h_+ & h_\times & 0 \\ h_\times & -h_+ & 0 \\ 0 & 0 & 0 \end{pmatrix} \cos\left[\omega\left(t - \frac{z}{c}\right)\right] \tag{3.20}$$

or, more simply,

$$h_{ab}^{TT}(t,z) = \begin{pmatrix} h_+ & h_\times \\ h_\times & -h_+ \end{pmatrix} \cos\left[\omega\left(t - \frac{z}{c}\right)\right] \tag{3.21}$$

h_+ and $h_\times$ are called respectively the "plus" and "cross" polarization amplitudes of the gravitational wave.

A way exists to bring any solution to the homogeneous wave equation, that satisfies the De Donder gauge, in the transverse-traceless gauge. This is done by means of a certain projector. To begin with, one introduces the symmetric tensor:

$$P_{ij}(\hat{n}) = \delta_{ij} - n_i n_j \tag{3.22}$$

where δ_{ij} is the 3x3 identity tensor. Then, through P_{ij} one can construct the projector:

$$\Lambda_{ij,kl} = P_{ik}P_{jl} - \frac{1}{2}P_{ij}P_{kl} \tag{3.23}$$

It verifies several properties: it is transverse on all indices (i.e. $n^i\Lambda_{ij,kl} = 0 = n^j\Lambda_{ij,kl}$ etc.), $\Lambda_{ii,kl} = \Lambda_{ij,kk} = 0$, $\Lambda_{ij,kl}\Lambda_{kl,mn} = \Lambda_{ij,mn}$ (which defines projectors) and it is symmetric under the symultaneous exchange $(i,j) \leftrightarrow (k,l)$. Using this projector, one can

bring a solution in the transverse-traceless gauge:

$$h_{ij}^{TT} = \Lambda_{ij,kl} h_{kl} \tag{3.24}$$

This is still a solution, since the $h_{\mu\nu}$ on the right hand side solves the homogeneous equation in the De Donder gauge. The next step involves solving equation (3.16) in a linearized theory. This means that the gravitational field generated by the source is assumed to be sufficiently weak, so that one can expand it in flat space-time. Therefore, the typical velocities inside the source are small, if compared to c. An example of a source, which shall be used later on, is a gravitationally-bound two-body system. In such a system the small velocities condition implies that the gravitational field is weak: through the virial theorem $2K + U = 0$, where K is the kinetic energy and U is the gravitational potential energy, therefore, using the reduced mass $\mu = \frac{m_1 m_2}{m_1 + m_2}$:

$$\frac{1}{2}\mu v^2 = \frac{1}{2}\frac{G\mu m}{r} \implies \frac{v^2}{c^2} = \frac{2Gm}{c^2 r} = \frac{R_S}{r} \tag{3.25}$$

R_S is called the total mass' (m) Schwarzschild radius. It can be easily seen then that a weak gravitational field, i.e. $\frac{R_S}{r} \ll 1$, implies $v \ll c$. In systems where the dynamics are determined by non-gravitational forces, weak-field expansion and low-velocity expansion are independant. Therefore, weak-field approximations with arbitrary velocities shall be examined and they shall be expanded in powers of $\frac{v}{c}$ and then organized in a multipole expansion, of which the lowest-order term shall be analyzed.

The starting point is equation (3.16) in the De Donder gauge. The solution will be sought through the Green function method: using $\mathscr{G}(x - x')$, which solves the equation:

$$\Box_x \mathscr{G}(x - x') = \delta^4(x - x') \tag{3.26}$$

one can write the solution to

$$\Box \bar{h}_{\mu\nu} = -\frac{16\pi G}{c^4} T_{\mu\nu} \tag{3.27}$$

as

$$\bar{h}_{\mu\nu} = -\frac{16\pi G}{c^4}\int d^4x' \mathscr{G}(x-x')T_{\mu\nu}(x') \tag{3.28}$$

This solution depends on the equation's boundary conditions and on the Green function one chooses to use. The Green function that is chosen is the retarded Green function

$$G_{ret}(x-x') = -\frac{1}{4\pi|\vec{x}-\vec{x'}|}\delta(x^0_{ret}-x'^0) \tag{3.29}$$

where $x^0_{ret} = ct_{ret} = c\left(t - \frac{|\vec{x}-\vec{x'}|}{c}\right)$. Therefore the solution takes on the form

$$\bar{h}_{\mu\nu}(\vec{x},t) = \frac{4G}{c^4}\int d^3x' \frac{1}{|\vec{x}-\vec{x'}|}T_{\mu\nu}(t_{ret},\vec{x'}) \tag{3.30}$$

Outside the source, this solution can be put in the transverse-traceless gauge by using **??**1.24), obtaining:

$$h^{TT}_{ij}(t,\vec{x}) = \frac{4G}{c^4}\Lambda_{ij,kl}(\hat{n})\int d^3x' \frac{1}{|\vec{x}-\vec{x'}|}T_{kl}(t_{ret},\vec{x'}) \tag{3.31}$$

where $\hat{n} = \hat{x}$. The elimination of the $T_{0\mu}$ and $T_{\mu 0}$ components of the matter energy-momentum tensor from this relation is done thanks to the continuity equation $\partial^\nu T_{\mu\nu} = 0$. Denoting by d the typical radius of the source and using $|\vec{x}| = r$, one can expand $|\vec{x}-\vec{x'}|$ for $r \gg d$ as:

$$|\vec{x}-\vec{x'}| = r - \vec{x'}\cdot\hat{n} + O\left(\left(\frac{d}{r}\right)^2\right) \tag{3.32}$$

Therefore, at large distances from the source, neglecting terms of order r^{-2} or higher,

$$h^{TT}_{ij}(t,\vec{x}) = \frac{4G}{c^4}\Lambda_{ij,kl}(\hat{n})\int d^3x'\ T_{kl}\left(t - \frac{r}{c} + \frac{\vec{x'}\cdot\hat{n}}{c},\vec{x'}\right) \tag{3.33}$$

By writing T_{kl} by means of its Fourier transform, one can relate the expression for the irradiated energy per solid angle

$$\frac{dE}{d\Omega} = \frac{r^2c^3}{32\pi G}\int_{-\infty}^{\infty} dt\ \dot{h}^{TT}_{ij}\dot{h}^{TT}_{ij} \tag{3.34}$$

where $\dot{h}_{ij}^{TT} = \partial_t h_{ij}^{TT}$, to the energy-momentum tensor itself. The inverse Fourier transform of T_{kl} is:

$$T_{kl}(t,\vec{x}) = \int \frac{d^4k}{(2\pi)^4} \tilde{T}_{kl}\left(\omega,\vec{k}\right)\ e^{\left(-i\omega t + i\vec{k}\cdot\vec{x}\right)} \tag{3.35}$$

then:

$$\begin{aligned}
&\int d^3x'\ T_{kl}\left(t - \frac{r}{c} + \frac{\vec{x'}\cdot\hat{n}}{c}, \vec{x'}\right) = \\
&\int d^3x' \int \frac{d\omega}{2\pi c}\frac{d^3k}{(2\pi)^3}\tilde{T}_{kl}\left(\omega,\vec{k}\right)\ e^{-i\omega\left(t-\frac{r}{c}\right)}\ e^{i\left(\vec{k}-\frac{\omega\hat{n}}{c}\right)\cdot\vec{x'}} = \\
&= \int \frac{d\omega}{2\pi c}\frac{d^3k}{(2\pi)^3}\tilde{T}_{kl}\left(\omega,\vec{k}\right)\ e^{-i\omega\left(t-\frac{r}{c}\right)}\,(2\pi)^3\,\delta^3\left(\vec{k} - \frac{\omega\hat{n}}{c}\right) = \\
&= \int \frac{d\omega}{2\pi c}\tilde{T}_{kl}\left(\omega,\frac{\omega\hat{n}}{c}\right)\ e^{-i\omega\left(t-\frac{r}{c}\right)}
\end{aligned} \tag{3.36}$$

Therefore:

$$h_{ij}^{TT}(t,\vec{x}) = \frac{1}{r}\frac{4G}{c^5}\Lambda_{ij,kl}(\hat{n})\int_{-\infty}^{\infty}\frac{d\omega}{2\pi}\ \tilde{T}_{kl}\left(\omega,\frac{\omega\hat{n}}{c}\right)\ e^{-i\omega\left(t-\frac{r}{c}\right)} \tag{3.37}$$

The Fourier components of the matter energy-momntum tensor tend to become large at a typical value ω_s, at which the mass within the source has a bulk movement with a velocity $v_s \sim \omega_s d$. This form for the solution is valid for any assumption on v_s, so it is valid in both relativistic and non-relativistic situations. By inserting (3.37) into (3.34), one obtains:

$$\frac{dE}{d\Omega} = \frac{G}{2\pi^2 c^7}\Lambda_{ij,kl}(\hat{n})\int_0^{\infty} d\omega\ \omega^2\ \tilde{T}_{ij}\left(\omega,\frac{\omega\hat{n}}{c}\right)\ \tilde{T}_{kl}^{*}\left(\omega,\frac{\omega\hat{n}}{c}\right) \tag{3.38}$$

where $\tilde{T}_{ij}\left(-\omega,-\vec{k}\right) = \tilde{T}_{ij}^{*}\left(\omega,\vec{k}\right)$ has been used and the right hand term indicates the complex conjugate of $\tilde{T}_{ij}$. Therefore, the energy spectrum is:

$$\frac{dE}{d\omega} = \frac{G\omega^2}{2\pi^2 c^7}\int d\Omega\ \Lambda_{ij,kl}(\hat{n})\,\tilde{T}_{ij}\left(\omega,\frac{\omega\hat{n}}{c}\right)\ \tilde{T}_{kl}^{*}\left(\omega,\frac{\omega\hat{n}}{c}\right) \tag{3.39}$$

3.2 Gravitational Waves in a small velocities approximation

Now that the problem has been solved for an arbitrary velocity, one can analyse it for velocities small if compared to the speed of light. Using the source characteristic frequency ω_s and its radius d, the velocities within the source will be of order $v_s = \omega_s d$. The frequency of the radiation will also be of order $\omega \sim \omega_s$, therefore, in terms of $\lambda\!\!\!^{-} = \frac{c}{\omega} \sim c\,\frac{d}{v}$, the small velocities condition becomes:

$$\lambda\!\!\!^{-} \gg d \tag{3.40}$$

In this case one can neglect the internal motions of the source, in favour of their lowest-order expansion. To do so, one needs to write (3.33) in terms of T_{kl}'s Fourier transform:

$$h_{ij}^{TT}(t,\vec{x}) = \frac{1}{r}\frac{4G}{c^4}\Lambda_{ij,kl}(\hat{n})\int d^3x' \int \frac{d^4k}{(2\pi)^4}\tilde{T}_{kl}\left(\omega,\vec{k}\right)\, e^{-i\omega\left(t-\frac{r}{c}+\vec{x'}\cdot\frac{\hat{n}}{c}\right)+i\vec{k}\cdot\vec{x'}} \tag{3.41}$$

Since the source is non-relativistic, its frequency will peak around ω_s, with $\omega_s d \ll c$. The matter energy momentum tensor is zero outside the source, therefore, the integral is restricted to $|\vec{x'}| \leq d$ and the dominant contribution will come from frequencies that satisfy:

$$\frac{\omega}{c}\vec{x'}\cdot\hat{n} \lesssim \frac{\omega_s d}{c} \ll 1 \tag{3.42}$$

Expanding the exponential term to first-order, one gets:

$$e^{-i\omega\left(t-r/c+\vec{x'}\cdot\hat{n}/c\right)} \;\approx\; e^{-i\omega(t-r/c)}\left[1-i\frac{\omega}{c}x'^j n_j\right] \tag{3.43}$$

While expanding the matter energy tensor, one gets:

$$T_{kl}\left(t-\frac{r}{c}+\frac{\vec{x'}\cdot\hat{n}}{c},\vec{x'}\right) \approx T_{kl}\left(t-\frac{r}{c},\vec{x'}\right)+\frac{x'^j n_j}{c}\partial_0 T_{kl}\left(t-\frac{r}{c},\vec{x'}\right) \tag{3.44}$$

Now, by defining the momenta of the stress tensor T^{ij},

$$\begin{aligned} S^{ij}(t) &= \int d^3x\, T^{ij}(t,\vec{x}) \\ S^{ij,k}(t) &= \int d^3x\, T^{ij}(t,\vec{x}) x^k \end{aligned} \tag{3.45}$$

etc. (higher order momenta are defined in the same way, by adding additional x terms to the integral), one can write (3.41) as:

$$h_{ij}^{TT}(t,\vec{x}) \approx \frac{1}{r}\frac{4G}{c^4}\Lambda_{ij,kl}(\hat{n})\left[S^{kl}\left(t-\frac{r}{c}\right)+\frac{1}{c}n_m\dot{S}^{kl,m}\left(t-\frac{r}{c}\right)\right] \tag{3.46}$$

From the momenta's definitions, one can see that $S^{kl,m}$ is an object that adds a factor of order $O(d)$ to S^{kl}. Therefore, $\dot{S}^{kl,m}$ is a term of order $O(\omega_s d) \sim O(v)$ with respect to S^{kl}, allowing the term $n_m\dot{S}^{kl,m}$ to be seen as the $O(v/c)$ term of the expansion.
From the momenta of T^{ij}, one can derive objects more interesting from a physical point of view: the momenta of T^{00}, the energy density, and the momenta of T^{0i}, the linear momentum. The former are defined as

$$\begin{aligned} M(t) &= \frac{1}{c^2}\int d^3x\, T^{00}(t,\vec{x}) \\ M^i(t) &= \frac{1}{c^2}\int d^3x\, T^{00}(t,\vec{x}) x^i \\ M^{ij}(t) &= \frac{1}{c^2}\int d^3x\, T^{00}(t,\vec{x}) x^i x^j \\ M^{ijk}(t) &= \frac{1}{c^2}\int d^3x\, T^{00}(t,\vec{x}) x^i x^j x^k \end{aligned} \tag{3.47}$$

and so on, while the latter as:

$$\begin{aligned} P^i(t) &= \frac{1}{c}\int d^3x\, T^{0i}(t,\vec{x}) \\ P^{i,j}(t) &= \frac{1}{c}\int d^3x\, T^{0i}(t,\vec{x}) x^j \\ P^{i,jk}(t) &= \frac{1}{c}\int d^3x\, T^{0i}(t,\vec{x}) x^j x^k \end{aligned} \tag{3.48}$$

and so on. By inserting these terms into the continuity equation $\partial_\mu T^{\mu\nu} = 0$, one can obtain laws of conservation for them by evaluating the integral of this equation over a

finite volume V, larger than the source's volume, so that $T^{\mu\nu}$ vanishes at the boundary ∂V. By integrating the $\nu = 0$ equation $\partial_\mu T^{\mu 0} = 0$, that is $\partial_0 T^{00} = -\partial_i T^{0i} = 0$, one gets:

$$c\dot{M} = \int_V d^3x\, \partial_0 T^{00} = -\int_V d^3x\, \partial_i T^{0i} = -\int_{\partial V} T^{0i} dS_i = 0 \tag{3.49}$$

where in the last equation, the Gauss theorem has been used to obtain a surface integral from the volume integral. $c\dot{M} = 0$ means that mass is conserved: the mass loss from gravitational wave emission can be neglected in linearized theory, since it can be treated as a "source recoil" effect. Simlarly, one obtains the identity:

$$\begin{aligned} c\dot{M}^i &= \int_V d^3x\, x^i \partial_0 T^{00} = -\int_V d^3x\, x^i \partial_j T^{0j} = \\ &= \int_V d^3x \left(\partial_j x^i\right) T^{0j} = \int_V d^3x\, \delta^i_j T^{0j} = cP^i \end{aligned} \tag{3.50}$$

from which, using the other momenta of T^{00} and T^{0i}, one can obtain the identities:

$$\begin{aligned} \dot{M}^{ij} &= P^{i,j} + P^{j,i} \\ \dot{P}^i &= 0 \\ \dot{P}^{i,j} &= S^{ij} \end{aligned} \tag{3.51}$$

$\dot{P}^i = 0$ means that the source's total linear momentum is conserved, if one neglects source recoil effects coming from loss of momentum from gravitational wave emission. From the third identity of 3.51, one obtains that $\dot{P}^{i,j} - \dot{P}^{j,i} = 0$, from the symmetry of S^{ij}. By exploiting this simmetry, one can get this final identity:

$$S^{ij} = \frac{1}{2}\ddot{M}^{ij} \tag{3.52}$$

Identity 3.52 can be used to obtain a more compact form for the $O(v/c)$ of the expansion, the quadrupole term 3.46:

$$\left[h^{TT}_{ij}(t,\vec{x})\right]_{\text{quad}} = \frac{1}{r}\frac{2G}{c^4}\Lambda_{ij,kl}(\hat{n})\ddot{M}^{kl}(t - r/c) \tag{3.53}$$

From the rotations group point of view, M^{kl} can be written as a traceless term plus a trace term, which vanishes when contracted with the Lambda tensor:

$$M^{kl} = \left(M^{kl} - \frac{1}{3}\delta^{kl}M_{ii}\right) + \frac{1}{3}\delta^{kl}M_{ii} \tag{3.54}$$

By introducing the quadrupole moment, defined as:

$$Q^{ij} = M^{ij} - \frac{1}{3}\delta_{ij}M_{kk} = \int d^3x\, \rho\,(t,\vec{x}) \left(x^i x^j - \frac{1}{3}r^2\delta^{ij}\right) \tag{3.55}$$

where $\rho = \frac{1}{c^2}T^{00}$ is the mass density. The quadrupole term therefore can be written as:

$$\left[h_{ij}^{TT}\,(t,\vec{x})\right]_{\text{quad}} = \frac{1}{r}\frac{2G}{c^4}\Lambda_{ij,kl}\,(\hat{n})\,\ddot{Q}_{kl}\,(t-r/c) = \frac{1}{r}\frac{2G}{c^4}\ddot{Q}_{ij}^{TT}\,(t-r/c) \tag{3.56}$$

The form for the quadrupole wave emitted in an arbitrary direction $\hat{n}$ can be derived by expressing the Lambda tensor by means of projectors (equation (3.23)): first, one uses the simple form of the projectors when $\hat{n} = \hat{z}$ and then one uses two rotations of angles θ and ϕ to bring the result in the desired direction. For an arbitrary matrix A_{kl}, the projection gives:

$$\Lambda_{ij,kl}A_{kl} = \left(P_{ik}P_{jl} - \frac{1}{2}P_{ij}P_{kl}\right)A_{kl} = (PAP)_{ij} - \frac{1}{2}P_{ij}\,\text{Tr}\,(PA) \tag{3.57}$$

If the projection is for direction $\hat{z}$, P has a matrix representation $P = \text{diag}(1,1,0)$, therefore:

$$\Lambda_{ij,kl}\ddot{M}_{kl} = \begin{pmatrix} \frac{\ddot{M}_{11}-\ddot{M}_{22}}{2} & \ddot{M}_{12} & 0 \\ \ddot{M}_{21} & -\frac{\ddot{M}_{11}-\ddot{M}_{22}}{2} & 0 \\ 0 & 0 & 0 \end{pmatrix} \tag{3.58}$$

From this, one can get the expressions for the plus and cross polarizations:

$$\begin{aligned} h_+ &= \frac{1}{r}\frac{G}{c^4}\left(\ddot{M}_{11} - \ddot{M}_{22}\right) \\ h_\times &= \frac{2}{r}\frac{G}{c^4}\ddot{M}_{12} \end{aligned} \tag{3.59}$$

By applying the two rotations to M_{ij}, one can bring it from a coordinate frame (x',y',z') where the direction of propagation $\hat{n}$ is $\hat{n} = \hat{x'} \times \hat{y'}$ back into the (x,y,z) frame where the direction of propagation is $\hat{z}$. In the "primed" frame, the polarization amplitudes take on the same form, i.e. M'_{ij} replaces M_{ij} and, by applying the rotations, one gets:

$$M_{ij} = R_{ik} R_{jl} M'_{kl} \tag{3.60}$$

where a rotation takes the form:

$$R_{ik} = \begin{pmatrix} \cos\phi & \sin\phi & 0 \\ -\sin\phi & \cos\phi & 0 \\ 0 & 0 & 1 \end{pmatrix} \begin{pmatrix} 1 & 0 & 0 \\ 0 & \cos\theta & \sin\theta \\ 0 & \sin\theta & -\sin\theta \end{pmatrix} \tag{3.61}$$

The final result for the quadrupole wave polarizations is:

$$\begin{aligned} h_+(t,\theta,\phi) &= \frac{G}{rc^4}\left[\left(\ddot{M}_{11}+\ddot{M}_{22}\right)\left(\cos^2\phi - \sin^2\phi\cos^2\theta\right) - \right. \\ &+ \ddot{M}_{33}\sin^2\theta - \ddot{M}_{12}\sin(2\phi)\left(1+\cos^2\theta\right) + \ddot{M}_{13}\sin\phi\sin(2\theta) + \\ &\left. + \ddot{M}_{23}\cos\phi\sin(2\theta)\right] \\ h_\times(t,\theta,\phi) &= \frac{G}{rc^4}\left[\left(\ddot{M}_{11}-\ddot{M}_{22}\right)\sin(2\phi)\cos\theta + 2\ddot{M}_{12}\cos(2\phi)\cos\theta - \right. \\ &\left. + 2\ddot{M}_{13}\cos\phi\sin\theta + 2\ddot{M}_{23}\sin\phi\sin\theta\right] \end{aligned} \tag{3.62}$$

Since the leading term in the expansion is a quadrupole term, one can easily admit that gravitational waves have no monopole or dipole terms. This is because they would depend respectively on M^i and P^i, which are conserved quantities. Therefore any contribution they would give to the expansion vanishes in linearized theory, where the conservation holds. They vanish also at higher expansion orders, because it can be proved that the absence of monopole and dipole radiation holds even when all non-linear terms of the expansion are taken into consideration.

3.3 Gravitational Waves in a Binary System

Now that the polarization amplitudes for the quadrupole term have been derived, they can be used to express the amplitudes of the gravitational wave emitted by a binary system. Such an object shall be modelled as consisting of two point masses m_1 and m_2, where the relative coordinate is performing a circular orbit. Initially, recoil effect shall be neglected, in order for it to be evaluated later. The non-vanishing components of M_{ij} for this system are:

$$\begin{aligned} M_{11} &= \mu R^2 \frac{1-\cos(2\omega_s t)}{2} \\ M_{22} &= \mu R^2 \frac{1+\cos(2\omega_s t)}{2} \\ M_{12} &= -\frac{1}{2}\mu R^2 \sin(2\omega_s t) \end{aligned} \tag{3.63}$$

Therefore, inserting them in equation (3.62), one gets the polarization amplitudes:

$$\begin{aligned} h_+(t,\theta,\phi) &= \frac{4G\mu\omega_s^2 R^2}{rc^4}\left(\frac{1+\cos^2\theta}{2}\right)\cos(2\omega_s t_{\text{ret}}+2\phi) \\ h_\times(t,\theta,\phi) &= \frac{4G\mu\omega_s^2 R^2}{rc^4}\cos\theta\sin(2\omega_s t_{\text{ret}}+2\phi) \end{aligned} \tag{3.64}$$

where ω_s is the source's typical frequency and R its radius. From an observational point of view, the only radiation one can observe is the one emitted in the direction that points from the system towards the observer. The angle θ, therefore is the angle i between the normal to the orbit and the line of sight. The distance from the source r can be considered as constant, since one can neglect how the Earth's motion and the source's motion influence this distance in most cases. Moreover, the angle ϕ is fixed, so that one can shift the cosine and sine arguments so that $2\omega_s t + 2\phi \to 2\omega_s t$. Therefore, the observer can see gravitational waves amplitude of the form:

$$\begin{aligned} h_+(t) &= \frac{4G\mu\omega_s^2 R^2}{rc^4}\left(\frac{1+\cos^2 i}{2}\right)\cos(2\omega_s t_{\text{ret}}) \\ h_\times(t) &= \frac{4G\mu\omega_s^2 R^2}{rc^4}\cos i\sin(2\omega_s t_{\text{ret}}) \end{aligned} \tag{3.65}$$

If now one considers the system's equation of motion:

$$\ddot{\vec{r}} = -\frac{Gm}{|\vec{r}|^3}\vec{r} \tag{3.66}$$

where $\vec{r} = \vec{r_2} - \vec{r_1}$ is the relative coordinate and $m = m_1 + m_2$ is the total mass. If one approximates the orbit as circular, $v^2/R = Gm/R^2$ with $v = \omega_s R$, therefore Kepler's law gives:

$$\omega_s^2 = \frac{Gm}{R^3} \tag{3.67}$$

By using this result and the definition of the chirp mass:

$$M_c = \mu^{3/5} m^{2/5} \tag{3.68}$$

equation (3.64) becomes:

$$\begin{aligned} h_+(t) &= \frac{4}{r}\left(\frac{GM_c}{c^2}\right)^{5/3}\left(\frac{\pi f_{\rm gw}}{c}\right)^{2/3}\frac{1+\cos^2\theta}{2}\cos\left(2\pi f_{\rm gw} t_{\rm ret} + 2\phi\right) \\ h_\times(t) &= \frac{4}{r}\left(\frac{GM_c}{c^2}\right)^{5/3}\left(\frac{\pi f_{\rm gw}}{c}\right)^{2/3}\cos\theta\sin\left(2\pi f_{\rm gw} t_{\rm ret} + 2\phi\right) \end{aligned} \tag{3.69}$$

where $f_{\rm gw} = \omega_{\rm gw}/(2\pi)$, with $\omega_{\rm gw} = 2\omega_s$. The loss of energy due to the emission of gravitational waves shall be now taken into account. The source of the radiated energy is the total energy:

$$E_o = K + U = -\frac{Gm_1 m_2}{2R} \tag{3.70}$$

therefore, to compensate for the loss of energy, R must decrease over time, causing ω_s to increase. Over a sufficiently long time scale, this causes the system to coalesce. As long as $\dot{\omega}_s \ll \omega_s^2$, one can keep the quasi-circular motion approximation and use Kepler's first law to obtain:

$$\dot{R} = -\frac{2}{3}(\omega_s R)\frac{\dot{\omega}_s}{\omega_s^2} \tag{3.71}$$

One can obtain the radiated power per solid angle by dividing the total radiated energy per solid angle by the period T. Expressing it in terms of the polarization amplitudes

gives, in the quadrupole approximation:

$$\left(\frac{dP}{d\Omega}\right)_{\text{quad}} = \frac{r^2c^3}{16\pi G}\left(\dot{h}_+^2 + \dot{h}_\times^2\right) = \frac{2G\mu^2R^4\omega_s^6}{\pi c^5}g(\theta) \tag{3.72}$$

where $g(\theta) = \left(\frac{1+\cos^2\theta}{2}\right)^2 + \cos^2\theta$.

By using the chirp mass and ω_{gw}, this becomes:

$$\left(\frac{dP}{d\Omega}\right)_{\text{quad}} = \frac{2c^5}{\pi G}\left(\frac{GM_c\omega_{\text{gw}}}{2c^3}\right)^{10/3} g(\theta) \tag{3.73}$$

Integrating over a solid angle and using $d\Omega\sin\theta d\theta d\phi$, one gets the total radiated power:

$$P = \frac{32c^5}{5G}\left(\frac{GM_c\omega_{\text{gw}}}{2c^3}\right)^{10/3} \tag{3.74}$$

By using Kepler's first law, the equation for the orbital total energy gives:

$$E_o = -\left(\frac{G^2M_c^5\omega_{\text{gw}}^2}{32}\right)^{1/3} \tag{3.75}$$

and, since $P = -\frac{dE_o}{dt}$, one can obtain that:

$$\dot{f}_{\text{gw}} = \frac{96}{5}\pi^{8/3}\left(\frac{GM_c}{c^3}\right)^{5/3} f_{\text{gw}}^{11/3} \tag{3.76}$$

Solving this equation, one can see that f_{gw} becomes large at $t = t_c$, the time of coalescence. Using the time to coalescence $\tau = t_c - t$, the solution can be written as:

$$f_{\text{gw}}(\tau) = \frac{1}{\pi}\left(\frac{5}{256}\frac{1}{\tau}\right)^{3/8}\left(\frac{GM_c}{c^3}\right)^{-5/8} \tag{3.77}$$

This solution formally diverges, but since after the distance between the stars in the system has become lower than a critical value, they merge, this divergence is physically irrelevant. Using the reference value of a chirp mass, $M_c = 1.21M_\odot$, which refers to a

system of two stars with a mass of $1.4M_\odot$ each, the solution becomes:

$$f_{\rm gw}(\tau) \simeq 134 \text{ Hz} \left(\frac{1.21M_\odot}{M_c}\right)^{5/3} \left(\frac{1\ s}{\tau}\right)^{3/8} \tag{3.78}$$

From this, one can obtain, from a system where $M_c = 1.21M_\odot$ from two $1.4M_\odot$ masses, the radiation a few milliseconds from coalescence at 1 kHz frequency. So, even if such a frequency results in a separation radius of 33 km, typical of systems composed of neutron stars or black holes, which are far from point-like, one can still get useful information from them in this approximation.

The next objective is to express the polarization amplitudes of the gravitational waves emitted by a coalescing binary system, when the inner dynamics of the system are not neglected. In a quasi-circular orbits approximation on a plane (x,y), one can write a particle's motion as

$$\begin{aligned} x(t) &= R(t)\cos(\Phi(t)/2) \\ y(t) &= R(t)\sin(\Phi(t)/2) \end{aligned} \tag{3.79}$$

where $\Phi(t) = 2\int_{t_0}^{t} dt'\ \omega_s(t)$. So, now, the changes that one has to take account for, when calculating the quadrupole term for the wave amplitude when source dynamics are not neglected, are to replace the term $\omega_{\rm gw}t$ with $\Phi(t)$ in the arguments of the sine and cosine functions and the factor $\omega_{\rm gw}$ with $\omega_{\rm gw}(t)$ outside of the trigonometric functions. One can instead neglect the terms involving the time derivatives of $R(t)$ and $\omega_{\rm gw}(t)$ because the phase of the system's coalescence which is being analyzed, the inspiral phase, involves frequencies that are low enough to allow it: $\dot{R}$ is negligible if $\dot{\omega}_s \ll \omega_s^2$, which implies that $GM_c\omega_s/c^3 \ll 0.5$, for $M_c = 1.24M_\odot$, and therefore $f_{\rm gw} \ll 13$ kHz, which is always true in the inspiral phase. Therefore:

$$\begin{aligned} h_+(t) &= \frac{4}{r}\left(\frac{GM_c}{c^2}\right)^{5/3}\left(\frac{\pi f_{\rm gw}(t_{\rm ret})}{c}\right)^{2/3}\left(\frac{1+\cos^2 i}{2}\right)\cos\left[\Phi(t_{\rm ret})\right] \\ h_\times(t) &= \frac{4}{r}\left(\frac{GM_c}{c^2}\right)^{5/3}\left(\frac{\pi f_{\rm gw}(t_{\rm ret})}{c}\right)^{2/3}\cos i\sin\left[\Phi(t_{\rm ret})\right] \end{aligned} \tag{3.80}$$

By solving the differential equation for $f_{\rm gw}$, one can solve the integral for $\Phi(t)$ and

obtain:

$$\Phi(t) = -2\left(\frac{5GM_c}{c^3}\right)^{-5/8}\tau^{5/8} + \Phi_0 \tag{3.81}$$

Therefore, the polarization amplitudes can be expressed as a function of the time to coalescence τ, measured by the observer:

$$\begin{aligned} h_+(\tau) &= \frac{1}{r}\left(\frac{GM_c}{c^2}\right)^{5/4}\left(\frac{5}{c\tau}\right)^{1/4}\left(\frac{1+\cos^2 i}{2}\right)\cos\left[\Phi(\tau)\right] \\ h_\times(\tau) &= \frac{1}{r}\left(\frac{GM_c}{c^2}\right)^{5/4}\left(\frac{5}{c\tau}\right)^{1/4}\cos i\ \sin\left[\Phi(\tau)\right] \end{aligned} \tag{3.82}$$

It can be seen from these equations that both frequencies and amplitudes increase as the system's coalescence draws closer: such a behaviour is referred to as *chirping*, because of its similarity to the chirping of a bird.

3.4 Propagation of a Gravitational Wave from a binary system to an observer

3.4.1 A small introduction to FRWL Cosmology

The propagation of gravitational waves over distances long enough that the expansion of the universe during the propagation towards the detector has to be taken into account, will now be considered. Most detectors can in fact detect coalescences at distances in the Gpc range and beyond, therefore such an analysis is of great importance if one wants to understand gravitational wave astronomy to a greater extent. To begin with, some notions of cosmology shall be recalled, in order to define important parameters such as redshift and luminosity distance.

On the Gpc scale, the universe can be approximated as homogeneous and isotropic and can be described by using the Friedmann-Robertson-Walker-Lemaitre (FRWL) metric:

$$ds^2 = g_{\mu\nu}dx^\mu dx^\nu = -c^2dt^2 + a^2(t)\left[\frac{dr^2}{1-kr^2} + r^2d\theta^2 + r^2\sin^2\theta\ d\phi^2\right] \tag{3.83}$$

where $a(t)$, an a-dimensional function, is called the scale factor and can be determined by using the metric as a solution to the Einstein equation and solving the resulting Friedmann equations. They depend on the cosmological model one has assumed for the universe's energy-momentum tensor. It is going to be assumed that one has solved those equations and found $a(t)$: an alternative method to describe a through a Taylor series expansion shall be discussed later. k is the called the curvature of the universe: $k = 0$ means a flat universe, $k = 1$ a closed universe, $k = -1$ an open universe. The metric's coordinates are called co-moving: a test mass initially at rest in the FRWL universe, will remain at a fixed value of its (r, θ, ϕ) coordinates, even if the universe is expanding. This result can be derived from the geodesic equation in the metric:

$$\frac{du^\mu}{ds} - \Gamma^\mu_{\alpha\beta} u^\alpha u^\beta = 0 \tag{3.84}$$

by computing the Christoffel symbols and taking the $\mu = 0$ component, one gets:

$$\frac{d|\vec{u}|}{dt} = -\frac{\dot{a}}{a}|\vec{u}| \tag{3.85}$$

So, if at the initial time t_0, $|\vec{u}(t_0)| = g_{ij} u^i u^j = 0$, u will remain zero at any subsequent time. The coordinates therefore stretch themselves, following the expansion of the universe, and any two objects, initially at zero velocity, will always retain their coordinate distance $r = r_2 - r_1$, even after a certain amount of time has passed. The only distance that has physical meaning is actually their spatial distance:

$$dr^2_{\text{ph}} = g_{ij} dx^i dx^j \tag{3.86}$$

If the first object is located at the origin, this distance is:

$$r_{\text{ph}}(t) = a(t) \int_0^r \frac{dr}{\sqrt{1 - kr^2}} \tag{3.87}$$

If a source emits a signal (e.g. a gravitational wave) at an instant t_{em}, the observer will receive it at t_{ob}: the signal will follow a light-type geodesic and therefore $ds^2 = 0$. This

gives:

$$\int_{t_{\rm em}}^{t_{\rm ob}} \frac{c\,dt}{a(t)} = \int_0^r \frac{dr}{\sqrt{1-kr^2}} \tag{3.88}$$

If a second wave is emitted at $t_{\rm em}+\Delta t_{\rm em}$, it will be observed at $t_{\rm ob}+\Delta t_{\rm ob}$, while the right hand term will stay the same, since source and observer are at a fixed co-moving distance:

$$\int_{t_{\rm em}+\Delta t_{\rm em}}^{t_{\rm ob}+\Delta t_{\rm ob}} \frac{c\,dt}{a(t)} = \int_0^r \frac{dr}{\sqrt{1-kr^2}} \tag{3.89}$$

By subtracting these last two equations, one finds, at linear order, that:

$$\Delta t_{\rm ob} = \frac{a\left(t_{\rm ob}\right)}{a\left(t_{\rm em}\right)}\Delta t_{\rm em} \tag{3.90}$$

The right hand term allows to define an important parameter, the redshift z of the source, as:

$$1+z = \frac{a\left(t_{\rm ob}\right)}{a\left(t_{\rm em}\right)} \tag{3.91}$$

through which one can express the time dilation between the source ($t_{\rm em}$ shall from now on be referred to as the source's time t_s) and the observer clocks:

$$dt_{\rm ob} = (1+z)dt_s \tag{3.92}$$

and the relationship between the frequencies and wavelengths measured in both frames:

$$\begin{aligned} f_{\rm ob} &= \frac{f_s}{1+z} \\ \lambda_{\rm ob} &= (1+z)\lambda_s \end{aligned} \tag{3.93}$$

In order to define the luminosity distance in a FRWL metric, one needs to introduce the energy flux $\mathscr{F}$ (energy per unit area and unit time) measured in the observer's frame and the source's luminosity L, which is the power it radiates in its rest frame:

$$\begin{aligned} L &= \frac{dE_s}{dt_s} \\ \mathscr{F} &= \frac{L}{4\pi d_L^2} \end{aligned} \tag{3.94}$$

d_L is the luminosity distance of the source. In order to relate it with the source's redshift, one can observe that:

$$\frac{dE_{\text{ob}}}{dt_{\text{ob}}} = \frac{1}{(1+z)^2}\frac{dE_s}{dt_s} \tag{3.95}$$

and that at t_{ob}, the radiation will spread over the detector, describing a sphere of area $4\pi a^2(t_{\text{ob}})\, r^2$, therefore:

$$\mathscr{F} = \frac{L}{4\pi a^2(t_{\text{ob}})\, r^2 (1+z)^2} \implies d_L(z) = a(t_{\text{ob}})\, r\,(1+z) \tag{3.96}$$

In order to express d_L as a function of redshift, one needs to know $a(t)$. If z is small, one can perform a Taylor series expansion of a as:

$$\frac{a(t)}{a(t_0)} = 1 + H_0(t-t_0) - \frac{1}{2}q_0 H_0^2 (t-t_0)^2 + o((t-t_0)^2) \tag{3.97}$$

where t_{ob} has been set as the present time t_0 and the cosmographical parameters H (the Hubble parameter) and q (the deceleration parameter) are defined as:

$$H(t) = \frac{\dot{a}(t)}{a(t)} \tag{3.98}$$

$$q(t) = -\frac{a(t)\ddot{a}(t)}{\dot{a}^2(t)} \tag{3.99}$$

and are calculated at the time t_0. Using the relation between a and z, this expansion can be expressed by means of the latter and one can find the $d_L(z)$ as:

$$d_L(z) = \frac{c}{H_0}\left[z + \frac{1}{2}(1-q_0)z^2\right] + o(z^3) \tag{3.100}$$

The first term gives the Hubble law $z = d_L\frac{H_0}{c}$, which gives a proportionality between redshifts and distances, while higher order terms are corrections to this law for sufficiently small z. One can derive a more explicit relation, which is valid for any value of z, by setting the curvature, e.g $k = 0$, and differentiating the relation between a and z:

$$\frac{dt}{a(t)} = -\frac{1}{a(t_0)}\frac{dz}{H(z)} \implies a(t_0)r = c\int_0^z \frac{dz'}{H(z')} \tag{3.101}$$

where r has been obtained from equation (1.88). Finally, one gets:

$$d_L(z) = c(1+z)\int_0^z \frac{dz'}{H(z')} \tag{3.102}$$

The Hubble parameter can be obtained if one knows the luminosity distance: therefore $d_L(z)$ can be used to explore the expansion history of the universe. To find $d_L(z)$ one needs to know $\mathscr{F}$ and L. $\mathscr{F}$ can be measured by the observer, while L needs to be known from the absolute luminosity of the source, which is possible when it is a "standardized candle". The redshift can be found from the redshift of the source's spectral lines. The following section will therefore explain a way to treat coalescing binary systems with gravitational wave emission as standardized candles. By using standardized candles like Cepheid variables (up to 600 Mpc) and type Ia Supernovae (above 600 Mpc), it has been possible to find $H_0 = 73 \pm 3$ km s^{-1} Mpc^{-1} and $q_0 = -0.74 \pm 0.18$.

3.4.2 Propagation of Gravitational Waves through a FRWL universe

The next step is to find how the waveform produced by a coalescing binary propagates through a FRWL universe. The calculations will be performed in the local wave zone, i.e. the distance from the source is large enough that the waves propagate with a $1/r$ behaviour, but small enough to neglect the expansion of the universe and therefore consider $a(t)$ as a constant. Using the Physical distance as the distance from the source, one can express the polarization amplitudes as:

$$h_+(t_s) = h_c\left(t_s^{\text{ret}}\right)\frac{1+\cos^2 i}{2}\cos\left[2\pi\int_0^{t_s^{\text{ret}}} dt_s'\, f_{\text{gw}}^{(s)}\left(t_s'\right)\right] \tag{3.103}$$

$$h_\times(t_s) = h_c\left(t_s^{\text{ret}}\right)\cos i \sin\left[2\pi\int_0^{t_s^{\text{ret}}} dt_s'\, f_{\text{gw}}^{(s)}\left(t_s'\right)\right] \tag{3.104}$$

$$h_c\left(t_s^{\text{ret}}\right) = \frac{4}{a\left(t_{\text{em}}\right)r}\left(\frac{GM_c}{c^2}\right)^{5/3}\left(\frac{\pi f_{\text{gw}}^{(s)}\left(t_s^{\text{ret}}\right)}{c}\right)^{2/3} \tag{3.105}$$

where r is the co-moving distance and the retarded time is measured by the source's clock. By using the time to coalescence measured by the source τ_s, one can express the

wave frequency as:

$$f_{\mathrm{gw}}^{(s)}(\tau_s) = \frac{1}{\pi}\left(\frac{5}{256}\frac{1}{\tau_s}\right)^{3/8}\left(\frac{GM_c}{c^3}\right)^{-5/8} \tag{3.106}$$

In order to find how the waveform propagates through the FRWL universe over cosmological distances, one could solve the same problem for a scalar field wave equation, which has an easier mathematical approach, and then substitute the gravitational wave tensor field in the solution. The wave equation one has to solve is always $\Box\psi = 0$, but this time the Dalembertian operator is:

$$\Box = \frac{1}{\sqrt{-g}}\partial_\mu\left(\sqrt{-g}g^{\mu\nu}\partial_\nu\right) \tag{3.107}$$

Introducing the conformal time η as:

$$\eta = \int_0 t\frac{dt'}{a(t')} \tag{3.108}$$

so that $d\eta = dt/a(t)$, the solution will be assumed in the form:

$$\psi(r,\eta) = \frac{1}{r}\varphi(r,\eta) \tag{3.109}$$

The wave equation becomes:

$$\begin{aligned}
&\partial_\mu\left(\sqrt{-g}g^{\mu\nu}\partial_\nu\right)\psi = 0\\
&\qquad\Downarrow\\
&-\frac{1}{c^2}\partial_\eta\left[a^2(\eta)\,r^2\partial_\eta\psi\right] + \partial_r\left[a^2(\eta)\,r^2\partial_r\psi\right] = 0\\
&\qquad\Downarrow\\
&\partial_r^2\varphi - \varphi'' - 2\frac{a'}{a}\varphi' = 0
\end{aligned} \tag{3.110}$$

where $\frac{1}{c}\frac{\partial f}{\partial \eta} = f' \; \forall f$ and so on. The solution shall then be sought in the form:

$$\varphi(r,\eta) = \frac{1}{a(\eta)} g(r,\eta) \tag{3.111}$$

where g is obtained by solving the equation:

$$\partial_r^2 g - g'' + \frac{a''}{a} g = 0 \tag{3.112}$$

Assuming that the universe is matter-dominated, $a''/a \sim \eta^{-2}$, therefore one can write the solution g as:

$$g(r,\eta) \simeq e^{\pm i\omega(\eta - r/c)} \tag{3.113}$$

as long as one is allowed to neglect all η^{-2} terms in the equation: in this case the frequency ω will verify $\eta^2\omega^2 \gg 1$, that means that ω is large if compared to the general background scale of the space-time (geometrical optics approximation). Therefore the scalar field can be approximated as:

$$\psi(r,\eta) \simeq \frac{1}{ra(\eta)} g\left(\eta - \frac{r}{c}\right) \tag{3.114}$$

Since calculations are performed in the local wave zone, one can fix a at its t_0 value, by fixing $\eta = t$ at a certain time t. The result is that the solution shall take the form:

$$\psi(r,t) \simeq \frac{1}{ra(t_0)} e^{\pm i\omega(t - r/c)} \tag{3.115}$$

The same steps can be followed for the wave equation for a tensor field $h_{\mu\nu}$ in the geometrical optics approximation and, since the polarization amplitudes each on their own solve a scalar field wave equation independent of the other, one can say that they decouple: they do not mix among each other during the propagation. This results in them keeping the same form they had for an inspiraling binary system (equations (3.103)-(3.105)), but with h_c replaced by:

$$h_c\left(t_s^{\text{ret}}\right) = \frac{4}{a(t_0)\, r}\left(\frac{GM_c}{c^2}\right)^{5/3}\left(\frac{\pi f_{\text{gw}}^{(s)}\left(t_s^{\text{ret}}\right)}{c}\right)^{2/3} \tag{3.116}$$

The geometrical optics approximation here can be rewritten as $2\pi f_{\rm gw} \gg t_0^{-1}$, where one can treat t_0 as the present age of the universe. Since the only gravitational waves one can observe are the ones whose wavelength is smaller than the Hubble size of the universe, all binary systems that are analysed in this problem satisfy the geometrical optics approximation. $2\pi f_{\rm gw} \gg t_{\rm em}^{-1}$ is also satisfied, therefore the approximation holds during the whole propagation.

Finally, all equations found in the source frame shall be brought into the observer's frame. Since the redshift in f cancels the one in t,

$$\int_0^{t_s^{\rm ret}} dt'_s f_{\rm gw}^{(s)}\left(t'_s\right) = \int_0^{t_{\rm ob}^{\rm ret}} dt'_{\rm ob} f_{\rm gw}^{(\rm ob)}\left(t'_{\rm ob}\right) \tag{3.117}$$

equation (3.93) allows to write:

$$h_c\left(t_{\rm ob}^{\rm ret}\right) = \frac{4}{d_L(z)}(1+z)^{5/3}\left(\frac{GM_c}{c^2}\right)^{5/3}\left(\frac{\pi f_{\rm gw}^{(\rm ob)}\left(t_{\rm ob}^{\rm ret}\right)}{c}\right)^{2/3} \tag{3.118}$$

$$f_{\rm gw}^{(\rm ob)}\left(t_{\rm ob}^{\rm ret}\right) = \frac{1}{1+z}\frac{1}{\pi}\left(\frac{5}{256}\frac{1+z}{\tau_{\rm ob}}\right)^{3/8}\left(\frac{GM_c}{c^3}\right)^{-5/8} \tag{3.119}$$

where $\tau_{\rm ob} = (1+z)\tau_s$ is the time to coalescence measured by the observer. In terms of this time, the amplitudes become:

$$h_+\left(\tau_{\rm ob}\right) = h_c\left(\tau_{\rm ob}\right)\frac{1+\cos^2 i}{2}\cos\left[\Phi\left(\tau_{\rm ob}\right)\right] \tag{3.120}$$

$$h_\times\left(\tau_{\rm ob}\right) = h_c\left(\tau_{\rm ob}\right)\cos i \sin\left[\Phi\left(\tau_{\rm ob}\right)\right] \tag{3.121}$$

Introducing the redshifted chirp mass $\mathscr{M}_c$ as:

$$\mathscr{M}_c = (1+z)\mu^{3/5}m^{2/5} \tag{3.122}$$

one can write:

$$h_c(\tau_{\rm ob}) = \frac{4}{d_L(z)}\left(\frac{G\mathscr{M}_c}{c^2}\right)^{5/3}\left(\frac{\pi f_{\rm gw}^{(\rm ob)}(\tau_{\rm ob})}{c}\right)^{2/3} \tag{3.123}$$

$$\Phi(\tau_{\rm ob}) = -2\left(\frac{5G\mathscr{M}_c}{c^3}\right)^{-5/8}\tau_{\rm ob}^{5/8} + \Phi_0 \tag{3.124}$$

$$f_{\rm gw}^{(\rm ob)}(\tau_{\rm ob}) = \frac{1}{\pi}\left(\frac{5}{256}\frac{1}{\tau_{\rm ob}}\right)^{3/8}\left(\frac{G\mathscr{M}_c}{c^2}\right)^{-5/8} \tag{3.125}$$

$$\dot{f}_{\rm gw}^{(\rm ob)} = \frac{96}{5}\pi^{8/3}\left(\frac{G\mathscr{M}_c}{c^2}\right)^{5/3}\left[f_{\rm gw}^{(\rm ob)}\right]^{11/3} \tag{3.126}$$

If one can measure both polarization amplitudes and $\dot{f}_{\rm gw}^{(\rm ob)}$ with respect to a given value of $f_{\rm gw}^{(\rm ob)}$, they can obtain the angle i, the inclination of the source's orbit with respect to the line of sight, from the amplitudes' ratio and $\mathscr{M}_c$ from equation (3.126). This fixes every quantity in equations (3.120), (3.121) and (3.123), except $d_L(z)$, which can now be found from the measured value of one of the amplitudes. If one can also measure the redshift z, then they can use it to measure $H(z)$: the inspiraling binary system can therefore been used as a gravitational wave standardized candle or "standard siren".

3.5 Determination of the Hubble Parameter using standard sirens

By inverting equation (1.123), one can express the luminosity distance as:

$$d_L(z) = \frac{4}{h_c(\tau_{\rm ob})}\left(\frac{G\mathscr{M}_c}{c^2}\right)^{5/3}\left(\frac{\pi f_{\rm gw}^{(\rm ob)}(\tau_{\rm ob})}{c}\right)^{2/3} \tag{3.127}$$

Since the sources' typical redshift rarely goes beyond 1-2, the "small z" condition, that allows equation (1.100) to be approximated by its first order term, is satisfied and one can use the Hubble law to derive the so-called Hubble diagram, i.e. how luminosity distance is related to redshift, using the values for several known sources. As an example, see [35], one could assume h_c and M_c from the detector's sensitivity curve and the source's composition (what kinds of objects the source is made of) respectively (e.g.

for Neutron Stars, $h_c \simeq 10^{-22}$ and $M_c = 1.22\ M_\odot$), and know the frequency ranges and the source's electromagnetic redshift, so that all parameters in equation (3.127) are fixed. By applying a linear fit to the resulting redshift-distance couples, by following the law

$$d_L(z) = \frac{c}{H_0} z \tag{3.128}$$

one can easily obtain H_0 and the Hubble diagram.

Now a definition of the ISCO frequency shall be given. In the strong gravitational fields of binary systems, when the distance between the two objects becomes small enough, if one uses Schwarzschild geometry, there exists a minimum value for the radial distance, beyond which no stable circular orbits are allowed. In Schwarzschild coordinates, that is one chooses a metric so that:

$$ds^2 = -\left(1 - \frac{r_S}{r}\right) c^2 dt^2 - \left(1 - \frac{r_S}{r}\right)^{-1} dr^2 + r^2 d\theta^2 + r^2 \sin^2\theta d\phi^2 \tag{3.129}$$

where $r_S = \frac{2Gm}{c^2}$ is the system's Schwarzschild radius, this distance is called the ISCO radius and can be written as:

$$r_{ISCO} = \frac{6Gm}{c^2} \tag{3.130}$$

Slow-adiabatic inspiraling quasi-circular motions, that are the ones which have been analysed so far, for the system can only happen at distances $r \geq r_{ISCO}$, therefore no gravitational wave emission from the system can happen below r_{ISCO}, when the gravitational field becomes strong enough to cause the binary system's components to collapse onto each other. Using Kepler's third law, one can compute the ISCO frequency and obtain:

$$f_{ISCO} = \frac{c^3}{12\pi Gm\sqrt{6}} \tag{3.131}$$

The next step is to exploit the "standard siren" method in order to obtain constraints on an alternative theory's parameters. That is, one uses a different theory to describe either the binary system's gravitational dynamics or the propagation, in this case one might change the metric or the entire relativistic action and therefore modify the Einstein

equation.

A simple way to do so would be to change the gravitational potential within the binary system: from the standard Newtonian potential, one can create an "effective" Yukawa-like potential, like the one introduced in [45]:

$$\Phi_{\text{eff}}(r) = -\frac{GM\left(1+\sum_{k=1}^{n}\alpha_k e^{-r/r_k}\right)}{r} \tag{3.132}$$

The r_k terms is called the range of characteristic scale of the k-th correction to the Newtonian potential, which depends on what further interactions are involved:

$$r_k = \frac{\hbar}{m_k c} \tag{3.133}$$

m_k is the mass of the k-th interaction's fundamental particle: such a particle is introduced when one tries to unify Newtonian gravity with this interaction. The k couples (α_k, r_k) represent the alternative theory parameters one has to estimate. Actually, once the k-th characteristic particle has been identified: it could be either a point-like test particle within the system, so that its orbit is no inner than the ISCO, or a fundamental particle (e.g. the gravitational scalar field boson with a mass $m_k \sim 10^{-27} eV/c^2$, or, in a case more likely to the one that is being examined here, $10^{-13} eV/c^2 \lesssim m_k \lesssim 10^{-5} eV/c^2$, which corresponds to the mass that is expected to carry the correction term to the gravitational force), only the correspondent α_k has to be estimated. For the sake of simplicity, one could truncate the sum to its first term and write:

$$\Phi_{\text{eff}}(r) = -\frac{G_{\text{eff}}(r)M}{r} \tag{3.134}$$

$$G_{\text{eff}}(r) = G\left(1+\alpha_1 e^{-r/r_1}\right) \tag{3.135}$$

If $r \gg r_1$, the exponential term tends to 0 and one obtains the standard Newton potential; on the other hand, if $r \ll r_1$, one can use a Taylor series expansion:

$$G_{\text{eff}}(r) \approx G\left[1+\alpha_1\left(1-\frac{r}{r_1}\right)\right] \approx G(1+\alpha_1) \tag{3.136}$$

and therefore replace the universal gravitation constant with:

$$G_{\text{eff}} = G(1+\alpha) \tag{3.137}$$

in equations (3.123)-(3.127). If one uses the value for H_0 obtained using (3.128) and replaces $d_L(z)$ with its modified version, they will get a value for α, which shall fully identify the gravitational potential of the extended theory. An another way to get a value for α is to get d_L from the electromagnetic analysis of this standardized candle or from the host galaxy's luminosity distance and solve the resulting equation with α as an unknown. This potential represents the local variations from the strong equivalence principle the more general extended theory of gravity causes: in such a theory, the standard Newtonian potential has to be replaced by a modified potential like the one in equations (3.132) and (3.134),(3.135). The result is that local gravity depends on the system's Lagrangian, defining a "non-minimally coupled theory".

To end this chapter, the benefits of the use an alternative theory of gravity, as well as the possible purposes of the above defined effective potential theory, shall be briefly discussed.

3.6 Limits of General Relativity and benefits of a modified theory

General Relativity fails to explain the early universe because of its inflationary nature. To better introduce this, a brief outline of these limits shall be given in the form of the flatness problem, the horizon problem and the monopole problem [50].

- *The flatness problem* is related to the relationship between the curvature of the universe k and the total relative cosmological density Ω. The latter is defined as the sum of all relative cosmological density components within the cosmological model, each defined by equation (2.3). This relationship is expressed by the

Friedmann Hubble parameter equation:

$$1-\Omega(t) = -k\left(\frac{c}{H(t)a(t)R_0}\right)^2 \tag{3.138}$$

where R_0 is the universe curvature radius. R_0 can be defined through the concept of an objects angular size, i.e. the angle under which an observer would see the object if they were placed at the vertex of a right angle triangle where the galaxy diameter is one of the catheti, $\alpha_d = \frac{D}{R_0 \sin(r/R_0)}$ where D is the object diameter and r its distance from Earth. In a flat universe, $R = c/H_0$. The current absolute value of equation (3.138) left hand expression is circa 0.005, determined through CMB and Type Ia Supernovae analysis. The equation right hand term depends on what period of the universe evolution one is considering since each component relative density fraction value, its relationship with the scale factor and the scale factor evolution with respect to time change according to it. When the matter and radiation components were balanced (when the age of the universe was around $t_{rm} \ll 10^{10}$ years), equation (3.138) had the form:

$$1-\Omega(t) = \frac{(1-\Omega_0)a^2}{\Omega_{r,0} + a\Omega_{m,0}} \tag{3.139}$$

where the $\Omega_{c,0}$ are the present time values of each component relative cosmological density. The value of the left hand term at that time was $|1-\Omega(t_{rm})| \lesssim 2\cdot 10^{-6}$. It can be derived that the value of this term was also different during the time of first nucleosynthesis $\left(|1-\Omega(t_{nuc})| \lesssim 7\cdot 10^{-16}\right)$ and at the Planck time $t_P = 5\cdot 10^{-44}$ s $\left(|1-\Omega(t_P)| \lesssim 2\cdot 10^{-62}\right)$. The flatness problem consists in General Relativity lacking a model to explain this variability in the absolute discrepancy of the total cosmological relative density from 1 throughout the history of the universe through a physical mechanism instead of imposing specific conditions at each time, e.g. different values of relative cosmological density for each universe component.

- *The horizon problem* involves the universe anisotropy and homogeneity at large scales. If one considers two opposite points on the last scattering surface (the

surface of the universe at which the separation from light and matter happened, currently at an angular diameter distance of circa 12.8 Mpc), whose distance from an observer is, at the present time, given by:

$$d(t_0) = c\int_{t_{ls}}^{t_0} \frac{dt}{a(t)} \tag{3.140}$$

their distance from the observer will be 0.98 times the horizon distance (that is only circa 250 kpc larger than the last scattering surface distance), that is the maximum distance after which correlation between two space-time events is no longer possible, if they are separated by a 180° angle when observed from Earth. This distance depends on how wide the universe is at the time of measure. The horizon problem actually lies on those points' temperature discrepancy: even though those points cannot exchange light or either come into thermal equilibrium with each other, their temperature is the same (nowadays circa 2.73 K) within 30 μK. General Relativity lacks a physical model to explain why such a precise discrepancy existed at any time during the evolution of the universe.

- *The monopole problem* can be briefly summarized as the lack of magnetic monopoles within our present-day universe. According to the Grand Unification Theory of electro-magnetic interaction, introduced in the 1970s by Salam, Glashow and Weinberg, at a temperature of above 10^{28} K, which corresponds to an energy of above 10^{21} eV. The universe had such a temperature when it was only around 10^{-36} s old: at that time, according to the theory, electro-weak and electro-strong forces had not separated from each other yet. As the universe temperature dropped below 10^{28} K, a spontaneous loss of symmetry which created magnetic monopoles as point-like topological defects. Their number density was supposed to be around 10^{82} per cubic meter and their energy density was around 10^{103} eV per cubic meter. The issue is that, because of the energy density of electro-magnetic radiation decreasing as circa $(a(t))^{-4}$ and the energy density of magnetic monopoles decreasing as circa $(a(t))^{-3}$, monopoles should have energetically dominated the universe when it was only 10^{-16} s old. It can be clearly seen from observations that this is false: their relative cosmological density has

been estimated to be around 10^{-15}. Once again, General Relativity fails to explain why this is nowadays true.

Guth's inflationary theory succeeds at solving these problems by adding an additional term to the universe components: the cosmological constant Λ. This is done by modifying the Friedmann acceleration equation

$$\frac{\ddot{a}}{a} = -\frac{4\pi G}{3c^2}(\varepsilon + 3P) \tag{3.141}$$

where ε is the energy density and P is the pressure, and the Friedmann Hubble Parameter equation, by adding a term $\Lambda/3$ to the right hand of each equation. In this way, the scale factor solution is :

$$a(t) \propto e^{H(t_i)t} \tag{3.142}$$

If one supposed that the universe started expanding exponentially (or "inflating") at some t_i time during the period of radiation domination, and stopped doing so at some t_f time during the same period, they could use Guth's theory to solve the 3 problems. By comparing the value of $a(t)$ before and after the inflation, one gets:

$$\frac{a(t_f)}{a(t_i)} = e^N \tag{3.143}$$

where N is called the "number of e-foldings", defined as $N = H(t_i)(t_f - t_i)$. Using $t_i \sim 10^{-36}$ s, from the Grand Unification Theory, and $t_f = (N+1)t_i$, one could suppose $H(t)$ to be constant and equal to $H(t_i)$ during the inflation period, and obtain

$$\left|1 - \Omega(t_f)\right| = e^{-2N}\left|1 - \Omega(t_i)\right| \tag{3.144}$$

If one supposed $|1 - \Omega(t_i)| \sim 1$ and used the present-day value $|1 - \Omega(t_0)| \sim 0.005$, they could solve:

$$\left|1 - \Omega(t_f)\right| \leq 2 \cdot 10^{-54}(N+1) \tag{3.145}$$

and obtain that N has to be at least equal to 60 to match the present-day observations. This solves the flatness problem. To solve the horizon problem, one could use the

radiation dominated era evolution of $a(t) \propto t^{1/2}$ and compare the horizon distance at the beginning and end of inflation:

$$d_h(t_i) = ca(t_i) \int_0^{t_i} \frac{dt}{a(t_i)(t/t_i)^{1/2}} = 2ct_i \approx 6 \cdot 10^{-28} \text{ m} \tag{3.146}$$

$$d_h(t_f) = ce^N a(t_i) \left(\int_0^{t_i} \frac{dt}{a(t_i)(t/t_i)^{1/2}} + \int_{t_i}^{t_f} \frac{dt}{a(t_i)e^{H(t_i)(t-t_i)}} \right) = e^N c \left(2t_i + \frac{1}{H(t_i)} \right) \approx 15 \text{ m} \tag{3.147}$$

using $N = 65$. Therefore, using this same value of N and $a(t) \sim t^{2/3}$ during the matter dominated era after last scattering, one obtains a last scattering time value of $d_h(t_{ls}) \approx 800$ Mpc, easily solving the non-causal correlation between two antipodal points on the surface. Finally, in order to solve the monopole problem, one simply need to consider that their number density would be decreasing as $n_m \sim e^{-3H(t_i)t}$ during the inflation, starting from $n_m(t_i) \approx 10^{82}$ m^{-3}. Therefore, using the aforementioned N value and performing all calculations, one would get a present-day value of $n_m(t_0) \approx 2 \cdot 10^{-83}$ m^{-3}, which is as abysmally low as one would need to acknowledge their complete lack in our universe.

Now the benefits of the effective potential theory shall be discussed.
In addition to the three great problems which have been addressed earlier, General Relativity is also unable to properly explain deviation from expected orbits of planets and self-gravitating objects, as well as studying binary pulsar systems whose strong gravitational field is well above the weak field limit used in the previous sections of this chapter. The use of an effective potential theory in General Relativity tests like the two that have just been mentioned, but also in others such as gravitational lensing observation of distant galaxies, could allow to better constrain their parameters and understand their evolution and dynamics [45].

There exist various ways to estimate an effective potential theory's parameters. This thesis will be concerned with using data from actually observed Gravitational Wave sources, as an independent addition to the ones performed by observing pulsar binaries

and orbital deviations within planetary systems and galaxies.

Chapter 4

Statistical analysis

The goal of this chapter is to perform a statistical analysis for the modified gravitation theory parameters, described in chapter 3, by using distance-redshift relations like the ones in equations (3.127) and (3.128), through the use of actually observed sources data. The first analysis aims to follow the steps explained in [35] and, assuming a fixed Hubble parameter H_0, hypothesizing that it has been derived from gravitational waves emitted by several sources, i.e. binary systems, of which, components' masses, observed wave frequency, redshift and wave amplitudes are known. Once these quantities have been measured, one can use equation (3.127) to find the luminosity distance and then equation (3.128) to find H_0. By imposing that H_0's value is e.g. 69 Mpc km^{-1} s^{-1}, one can use that value to better understand what the boundaries on a theory's characteristic parameters can be. To this end, the theory's $d_L(z)$ relation has to be known. One case is the α effective potential Yukawa-like theory presented earlier in section 3.5. The relation, in that case, is simply:

$$d_L(z) = \frac{4}{h_c(\tau_{\text{ob}})}\left(\frac{G_{\text{eff}}\,\mathscr{M}_c(z)}{c^2}\right)^{5/3}\left(\frac{\pi f_{\text{gw}}^{(\text{ob})}(\tau_{\text{ob}})}{c}\right)^{2/3} \tag{4.1}$$

where G_{eff} is the effective potential described in equation (3.137), in order to find a range of values for α. The sources that are going to be used for this purpose are some of the ones contained in the GLADE (Galaxy List for the Advanced Detector Era) cat-

alogue, described in [52], which are contained in table 4.

Object Name(Catalogue)	d_L (Mpc)	z	f range (Hz)	max $\lvert\alpha\rvert$
05345097-6033379(2MASS XSC)	270 ± 16	0.061	30	$2.1 \cdot 10^{-3}$
09121957-6442494(2MASS XSC)	380 ± 22	0.083	34-35	$3.0 \cdot 10^{-3}$
03195178+1845338(2MASS XSC)	905 ± 151	0.19	465-500	$3.3 \cdot 10^{-4}$
SDSSJ084445.84+601519.9(HyperLEDA)	1399 ± 233	0.27	760-790	$5.6 \cdot 10^{-5}$
14433811+7449583(2MASS XSC)	819 ± 130	0.17	178-188	$8.3 \cdot 10^{-4}$
11385184+7106547(2MASS XSC)	678 ± 107	0.14	143-151	$1.2 \cdot 10^{-3}$
07250648+2412360(2MASS XSC)	313 ± 16	0.069	629-679	$3.3 \cdot 10^{-4}$
20248(HyperLEDA)	269 ± 14	0.060	511-552	$2.7 \cdot 10^{-4}$
SDSSJ094831.64+273508.2(HyperLEDA)	1709 ± 461	0.32	113-118	$1.2 \cdot 10^{-3}$
SDSSJ094321.65+325435.9(HyperLEDA)	1751 ± 432	0.33	115-119	$1.7 \cdot 10^{-2}$
11082886+4413131(2MASS XSC)	237 ± 14	0.056	25-26	$6.9 \cdot 10^{-3}$
12495659-0334315(2MASS XSC)	243 ± 14	0.055	26-27	$3.8 \cdot 10^{-4}$
3208315(HyperLEDA)	1081 ± 141	0.22	135-142	$1.2 \cdot 10^{-4}$
109313(HyperLEDA)	764 ± 99	0.16	80-84	$1.7 \cdot 10^{-3}$
112286(HyperLEDA)	559 ± 49	0.15	112-119	$6.0 \cdot 10^{-4}$
111039(HyperLEDA)	647 ± 57	0.14	100-104	$1.5 \cdot 10^{-3}$

Table 4.1: Luminosity distance, redshift, frequency and $|\alpha|$ data from selected GLADE catalogue objects. The frequency range is first roughly calculated by imposing d_L to be equal to the one contained inside the catalogue, that has been measured by using gravitational wave detection, then it is refined by imposing $|\alpha| \lesssim 10^{-3}$. The selected objects' redshifts, taken directly from the catalogue, have been calculated from the luminosity distance, by imposing H_0 to be 68 ± 2 km s^{-1} Mpc^{-1}. The redshift error is assumed to be around $1.5 \cdot 10^{-2}$ [52]. The luminosity distance has been calculated by using equation (3.127) and has an error that has been calculated via standard error propagation formulas. Note that the the error on the chirp mass has been obtained from an estimate of its measurement by present-day LIGO detectors as a 3% uncertainty, that is assumed to be the same as the frequency error. The value of α has been obtained by inverting equation 4.1 and imposing d_L to be the one in the second column.

Most sources have allowed to obtain $|\alpha|$ values within the $10^{-3} - 10^{-4}$ range. These values are coherent with the $|\alpha| \sim 10^{-3} - 10^{-4}$ expected limits, found by very long baseline interferometry observations and relativistic analysis of binary pulsars like [18]. It must be stressed that every extended theory measurement that is considered in this chapter, has to be considered as a prediction, since no actual measurement has yet been performed by any current mission. If a source's minimum $|\alpha|$ value is too incoherent with the expected ones, it shall be assumed that the source cannot be exploited in order to understand the differences between general relativity and this effective potential

gravitational theory.

The equation used in order to calculate source parameters from the value of the Hubble parameter at the present time (H_0), is the linear approximation of the Hubble law,

$$H_0 = \frac{cz}{d_L} \tag{4.2}$$

whose use is justified by the sources' low redshifts.

The idea that is exploited is that, if a GW source were to be detected at the object's redshift, that could be assumed as the host galaxy's redshift, what frequency range should it be detected at in order to allow for the α parameter to be in the accepted $10^{-3} \sim 10^{-4}$ range?

Now the reasons for choosing both the catalogue and the sources within it shall be discussed.

The GLADE catalogue, as stated within the article by compilers Dàlya et al., has been created by cross-matching five different catalogues (GWGC, HyperLEDA,2 Micron All Sky Survey Extended Catalogue or 2MASS XSC, 2MASS Photometric Redshift Catalogue or 2MPZ and the Sloan Digital Sky Survey Quasar Catalogue in its 12th Data Release or SDSS-DR12Q).

As stated by various articles (such as [38]), the use of a galaxy catalogue for the purpose of sources selection allows to increase the chance of detecting electro-magnetic counterparts to binary system coalescences (i.e. Short Hard Gamma Ray Burst events following Neutron Star coalescences). Those events are crucial to the measurement of the Hubble parameter, because they allow the measurement of the source redshift. Furthermore, their discovery can reduce the parameter space of Gravitational Wave search, therefore Gravitational Wave discovery efficiency can be increased. Furthermore, the use of galaxy catalogues can allow to perform accurate cosmological model simulations, from which one can e.g. obtain information about cosmology theories like the matter density of the universe. The GLADE catalogue sources cover a wide range of luminosity distances and have a good variety among galaxies, quasars and globular clusters, giving even another reason for its choice.

The sources chosen for analysis are the ones whose redshift has been derived from their luminosity distance, that has been measured by using gravitational waves propagation analysis (see chapter 3), imposing the Hubble parameter to be the one obtained by assuming General Relativity and a flat space cosmology, $H_0 = 70 \ \pm 2$ km s^{-1} Mpc^{-1}. These sources have been used because they are the ones that can be more easily cross-referenced with the other catalogues used to create GLADE, since it can be seen within the catalogue that their name also appears on at least one other catalogue. They can therefore be considered more reliable for analysis. Moreover, since the photometric redshift of a black hole coalescence is almost always nearly impossible to determine because such an event does not have an electro-magnetic counterpart, knowing the luminosity distance of the event is, within the error range, is, alongside angular astrophysical coordinates (Right Ascension and Declination), a very important way to locate a source and it also takes into account the evolution of the universe, since it depends on what cosmological model is used.

It shall now be discussed to what extent the Right Ascension and Declination data reported within the catalogue are to be considered reliable. By "reliable", one means whether they can actually be considered, within the uncertainty intervals, to be the actual, i.e. measurable via electro-magnetic signal acquisition, parallax methods etc., coordinates and whether the specific object's coordinates are within the current LIGO interferometers observation ranges.
The aforementioned uncertainty ranges can be assumed to be at best around 10 square degrees, if the source is simultaneously identified by 3 interferometers, but, the fewer the number of the interferometers is, the bigger this value can become. Therefore, the sources' coordinates have been compared with the coordinate uncertainty ranges for the sources detected by the aLIGO-VIRGO collaboration described in [55], in order to understand how accurately they can be considered to be within the current GW detectors' observation ranges. In table 4, each GLADE source has been associated with the closest source or sources from the GWTC catalogue created by the aLIGO-VIRGO collaboration, while in table 4 and figure 4 the properties of the reference GWTC sources are summarized.

Object Name(Catalogue)	RA (°)	DEC (°)	Closest GWTC sources (confidence area)
05345097-6033379(2MASS XSC)	84	-61	GW150914(50%)
09121957-6442494(2MASS XSC)	138	-65	GW150914(90%)
03195178+1845338(2MASS XSC)	50	19	GW151012(50%)
SDSSJ084445.84+601519.9(HyperLEDA)	131	60	GW151012(90%)
14433811+7449583(2MASS XSC)	221	75	GW170104(50%)
11385184+7106547(2MASS XSC)	175	71	GW170104(50%)
07250648+2412360(2MASS XSC)	111	24	GW170608(50%)
20248(HyperLEDA)	107	26	GW170608(50%)
SDSSJ094831.64+273508.2(HyperLEDA)	147	28	GW170729(90%)
SDSSJ094321.65+325435.9(HyperLEDA)	146	33	GW170729(90%)
11082886+4413131(2MASS XSC)	167	44	GW151226(90%)
12495659-0334315(2MASS XSC)	193	-4	GW151226(50%)
3208315(HyperLEDA)	29	-27	GW170809(50%)
109313(HyperLEDA)	24	-45	GW170809(50%)
112286(HyperLEDA)	61	-45	GW170814(50%)
111039(HyperLEDA)	48	-41	GW170814(50%)

Table 4.2: Most probable sources within the GWTC Catalogue with respect to proximity to the above discussed GLADE objects.The confidence areas are obtained from the aforementioned source for the GWTC catalogue and refer to statistics-based probability measurements, therefore the 50% confidence elliptic area is more narrow but refers to the object's closest neighbourhood.

As it can be seen by observing the results in the tables contained in this chapter, the analysis of several objects from the GLADE catalogue has allowed to find evidence for the possibility of justifying the previously discussed expected α value ranges for the effective G potential alternative theory described in chapter 3. Therefore, there appears to be evidence for the capability of current LIGO gravitational wave detectors to observe sources whose signal analysis can allow to estimate and verify alternative theories of gravity parameters.

Object Name	$\mathscr{M}_c(M_\odot)$	d_L(Mpc)	z
GW150914	28.6 ± 1.6	440 ± 160	0.09 ± 0.03
GW151012	15.2 ± 1.7	1080 ± 520	0.21 ± 0.09
GW170104	21.4 ± 2.0	990 ± 435	0.20 ± 0.08
GW170608	7.9 ± 0.2	320 ± 115	0.07 ± 0.02
GW170729	35.4 ± 5.3	2840 ± 1380	0.49 ± 0.20
GW151226	8.9 ± 0.3	450 ± 185	0.09 ± 0.04
GW170809	24.9 ± 1.9	1030 ± 360	0.20 ± 0.06
GW170814	24.1 ± 1.2	600 ± 185	0.12 ± 0.04

Table 4.3: Chirp mass, luminosity distance and redshift data for the GWTC sources used in table 4. The data have been taken from Abbott et al.'s article on the catalogue [55].

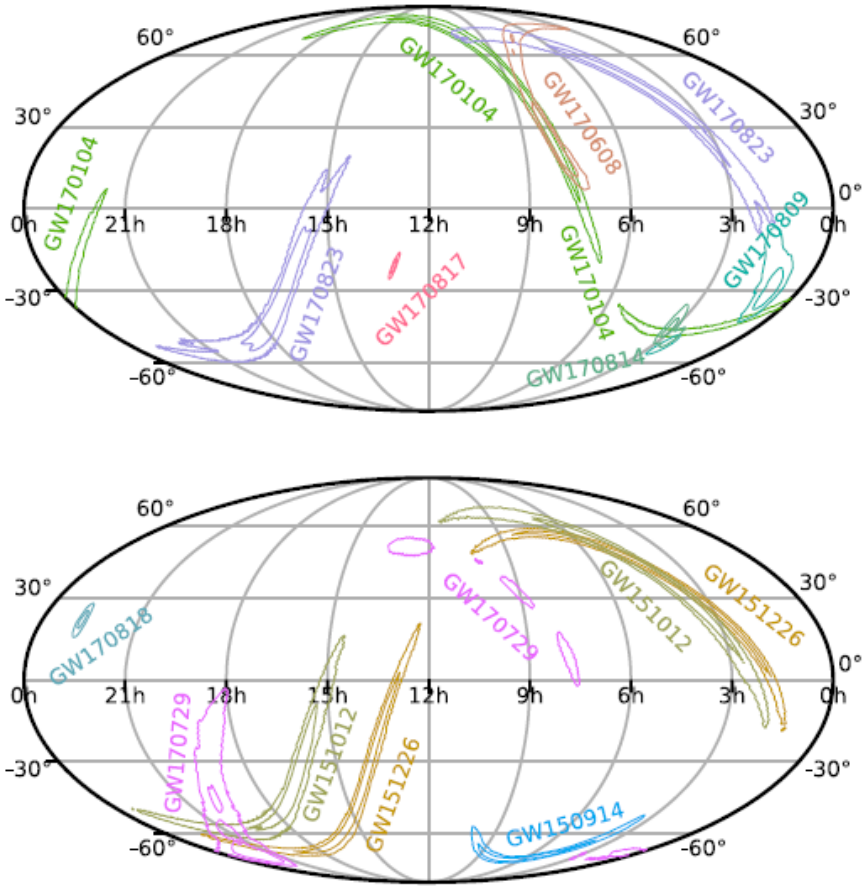

Figure 4.1: Right Ascension (measured in hours) and Declination data from sources in the GWTC catalogue. Each source has concentric elliptical confidence areas. The outer one is the 90% confidence area, while the inner one is the 50% confidence area.

Chapter 5

Conclusions and future perspectives

The objective of this thesis is the use of a candidate Gravitational Wave sources catalogue, the GLADE catalogue, to analyse the parameters of a modified theory of gravity through gravitational waves propagation analysis within this theory. The theory that has been analysed is a relatively simple one: an effective potential theory with a Yukawa-like evolution. The approximation to the first order term in a Taylor series approximation is justified by the source's large distance from the observer and further strengthened by the analysis of theoretical ranges for the α parameter and the use of those parameters to understand what frequency ranges should sources from the GLADE catalogue be observed at in order to justify their values. The use of GLADE sources has allowed to find frequency ranges to justify α values within the expected ones from very long baseline interferometers observations and relativistic analysis of binary pulsars. The selected sources from GLADE have been compared with the coordinate, redshift and luminosity distance intervals of GWTC sources, finding several sources within those error boundaries. This has allowed to conclude that it is very likely for gravitational waves from inspiraling binary black holes, the nature of GWTC sources, to be detected from objects within the GLADE catalogue, since several of

them lie within the aLIGO-VIRGO observational boundaries, since the expected frequency ranges lie within the scope of the aLIGO-VIRGO interferometers.
In the historical chapter, the use of gravitational waves as distance indicators has been motivated through the analysis of their benefits and of what achievements their study could fulfil, while in the theoretical one, the generation of gravitational waves and their propagation throughout the modified theory of gravitation framework has been developed and the benefits of alternative theories of gravity have been emphasized.
Finally some future perspectives shall be given:

- The use of space-detected sources, such as the ones found by the LISA interferometer, to further motivate the likelihood of finding gravitational wave emissions from inspiraling binary black holes within the GLADE catalogue, adding more sources to the candidates within the GLADE catalogue.

- The use of the modified theory of gravity to perform General Relativity tests on the propagation of gravitational waves from other sources within the observation ranges of the aLIGO-VIRGO interferometers

- Finally, one could do what has been done in chapters 3 and 4 for other alternative theories of gravity, such as scalar-tensor theories, in order to justify the constraints on their parameters through the analysis of observed gravitational waves emission from objects through the combined use of the GWTC and other catalogues.

Bibliography

[1]D. McLaughlin, "Pub. asp, 57, 69.. 1960", Stellar Atmospheres, 585 (1945).

[2]D Chalonge and L Divan, "La classification stellaire bcd: paramètre caractéristique du type spectral calibration en magnitudes absolues.", Astronomy and Astrophysics **23**, 69–79 (1973).

[3]G De Vaucouleurs and W. Pence, "Type i supernovae as cosmological clocks", The Astrophysical Journal **209**, 687–692 (1976).

[4]G De Vaucouleurs, "The extragalactic distance scale. i-a review of distance indicators-zero points and errors of primary indicators", The Astrophysical Journal **223**, 351–363 (1978).

[5]F. Pacini and M. Tarenghi, *Astronomical uses of the space telescope* (ESO, Geneva, 1979).

[6]B. F. Schutz, "Determining the hubble constant from gravitational wave observations", Nature **323**, 310–311 (1986).

[7]A Krolak and B. F. Schutz, "Coalescing binaries—probe of the universe", General Relativity and Gravitation **19**, 1163–1171 (1987).

[8]K. S. Thorne, S Hawking, and W Israel, *300 years of gravitation* (Cambridge University Press, Cambridge, England, 1987).

[9]M. Capaccioli, E. Cappellaro, M. della Valle, M. D'Onofrio, L. Rosino, and M. Turatto, "Distances of the virgo and coma clusters of galaxies through novae and supernovae", The Astrophysical Journal **350**, 110–118 (1990).

[10]G. Tammann and B Leibundgut, “Supernova studies. iv-the global value of h0 from supernovae ia and the peculiar motion of field galaxies”, Astronomy and Astrophysics **236**, 9–14 (1990).

[11]J. C. Wheeler and R. P. Harkness, “Type i supernovae”, Reports on Progress in Physics **53**, 1467 (1990).

[12]D. Branch and G. Tammann, “Type ia supernovae as standard candles”, Annual review of astronomy and astrophysics **30**, 359–389 (1992).

[13]D. L. Miller and D. Branch, “Type ia supernovae and cosmic peculiar velocities”, The Astronomical Journal **103**, 379–384 (1992).

[14]M. Hamuy, J. Maza, M. Phillips, N. B. Suntzeff, M Wischnjewsky, R. Smith, R Antezana, L. Wells, L. Gonzalez, P Gigoux, et al., “The 1990 calán/tololo supernova search”, The Astronomical Journal **106**, 2392–2407 (1993).

[15]A. Burrows, J. Hayes, and B. Fryxell, “On the nature of core collapse supernova explosions”, arXiv preprint astro-ph/9506061 (1995).

[16]L. Lindblom and G. Mendell, “Does gravitational radiation limit the angular velocities of superfluid neutron stars”, The Astrophysical Journal **444**, 804–809 (1995).

[17]E. E. Flanagan and S. A. Hughes, “Measuring gravitational waves from binary black hole coalescences. ii. the waves’ information and its extraction, with and without templates”, Physical Review D **57**, 4566 (1998).

[18]I. H. Stairs, Z. Arzoumanian, F. Camilo, A. G. Lyne, D. J. Nice, J. H. Taylor, S. E. Thorsett, and A. Wolszczan, “Measurement of relativistic orbital decay in the PSR B1534+12 binary system”, The Astrophysical Journal **1**, 314–333 (1998).

[19]N. Tanvir, “Cepheid standard candles”, arXiv preprint astro-ph/9812356 (1998).

[20]B. Allen and J. D. Romano, “Detecting a stochastic background of gravitational radiation: signal processing strategies and sensitivities”, Physical Review D **59**, 102001 (1999).

[21]M. Vallisneri, “Prospects for gravitational-wave observations of neutron-star tidal disruption in neutron-star–black-hole binaries”, Physical Review Letters **84**, 3519 (2000).

[22]T. Damour and A. Vilenkin, "Gravitational wave bursts from cusps and kinks on cosmic strings", Physical Review D **64**, 064008 (2001).

[23]V. Kalogera, R Narayan, D. N. Spergel, and J. Taylor, "The coalescence rate of double neutron star systems", The Astrophysical Journal **556**, 340 (2001).

[24]M. Kamionkowski and A. H. Jaffe, "Detection of gravitational waves from inflation", International Journal of Modern Physics A **16**, 116–128 (2001).

[25]C. Cutler and K. S. Thorne, "An overview of gravitational-wave sources", in *General relativity and gravitation* (World Scientific, 2002), pp. 72–111.

[26]M. McLaughlin, Z Arzoumanian, J. Cordes, D. Backer, A. Lommen, D. Lorimer, and A. Zepka, "Psr j1740+ 1000: a young pulsar well out of the galactic plane", The Astrophysical Journal **564**, 333 (2002).

[27]A. K. Inoue, R. Yamazaki, and T. Nakamura, "Near-infrared colors of gamma-ray burst afterglows and cosmic reionization history", The Astrophysical Journal **601**, 644 (2004).

[28]D. E. Holz and S. A. Hughes, "Using gravitational-wave standard sirens", The Astrophysical Journal **629**, 15 (2005).

[29]N. Kawai et al., *Gcn cric. 3937*, `http//www.mpe.mpg.de/~jcg/grbgen.html`, 2005.

[30]E. Liang and B. Zhang, "Model-independent multivariable gamma-ray burst luminosity indicator and its possible cosmological implications", The Astrophysical Journal **633**, 611 (2005).

[31]G. Stratta, R Perna, D Lazzati, F Fiore, L. Antonelli, and M. Conciatore, "Extinction properties of the x-ray bright/optically faint afterglow of grb 020405", Astronomy & Astrophysics **441**, 83–88 (2005).

[32]V. Bromm and A. Loeb, "High-redshift gamma-ray bursts from population iii progenitors", The Astrophysical Journal **642**, 382 (2006).

[33]G. Ghirlanda, G Ghisellini, and C Firmani, "Gamma-ray bursts as standard candles to constrain the cosmological parameters", New Journal of Physics **8**, 123 (2006).

[34]M. Maggiore, *Gravitational Waves, Volume 1: Theory and Experiments*, edited by Oxford University Press, Vol. 25, 20 (Oxford, 2008).

[35]S. Capozziello, M. De Laurentis, I. De Martino, and M. Formisano, "Coalescing binaries as possible standard candles", Astroparticle Physics **33**, 190–194 (2010).

[36]V. Faraoni and S. Capozziello, *Beyond einstein gravity: a survey of gravitational theories for cosmology and astrophysics* (Springer, 2011).

[37]D. J. Mortlock, S. J. Warren, B. P. Venemans, M. Patel, P. C. Hewett, R. G. McMahon, C. Simpson, T. Theuns, E. A. Gonzáles-Solares, A. Adamson, et al., "A luminous quasar at a redshift of z= 7.085", Nature **474**, 616–619 (2011).

[38]J Abadie, B. Abbott, R Abbott, T. Abbott, M Abernathy, T Accadia, F Acernese, C Adams, R Adhikari, C Affeldt, et al., "Implementation and testing of the first prompt search for gravitational wave transients with electromagnetic counterparts", Astronomy & Astrophysics **539**, A124 (2012).

[39]P. A. Ade, N Aghanim, C Armitage-Caplan, M Arnaud, M Ashdown, F Atrio-Barandela, J Aumont, C Baccigalupi, A. J. Banday, R. Barreiro, et al., "Planck 2013 results. xvi. cosmological parameters", Astronomy & Astrophysics **571**, A16 (2014).

[40]J.-M. Wang, P. Du, C. Hu, H. Netzer, J.-M. Bai, K.-X. Lu, S. Kaspi, J. Qiu, Y.-R. Li, F. Wang, et al., "Supermassive black holes with high accretion rates in active galactic nuclei. ii. the most luminous standard candles in the universe", The Astrophysical Journal **793**, 108 (2014).

[41]B. P. Abbott, R Abbott, T. Abbott, M. Abernathy, F Acernese, K Ackley, C Adams, T Adams, P Addesso, R. Adhikari, et al., "Binary black hole mergers in the first advanced ligo observing run", Physical Review X **6**, 041015 (2016).

[42]B. P. Abbott, R Abbott, T. Abbott, M. Abernathy, F Acernese, K Ackley, C Adams, T Adams, P Addesso, R. Adhikari, et al., "Gw151226: observation of gravitational waves from a 22-solar-mass binary black hole coalescence", Physical review letters **116**, 241103 (2016).

[43]J. L. Bernal, L. Verde, and A. G. Riess, "The trouble with h0", Journal of Cosmology and Astroparticle Physics **2016**, 019 (2016).

[44]P. S. Cowperthwaite, E. Berger, M Soares-Santos, J Annis, D Brout, D. Brown, E Buckley-Geer, S. Cenko, H. Chen, R Chornock, et al., "A decam search for an optical counterpart to the ligo gravitational-wave event gw151226", The Astrophysical Journal Letters **826**, L29 (2016).

[45]M. De Laurentis, O. Porth, L. Bovard, B. Ahmedov, and A. Abdujabbarov, "Constraining alternative theories of gravity using GW150914 and GW151226", Physical Review D **94**, 1–11 (2016).

[46]A. G. Riess, L. M. Macri, S. L. Hoffmann, D. Scolnic, S. Casertano, A. V. Filippenko, B. E. Tucker, M. J. Reid, D. O. Jones, J. M. Silverman, et al., "A 2.4% determination of the local value of the hubble constant", The Astrophysical Journal **826**, 56 (2016).

[47]B. Bécsy, P. Raffai, N. J. Cornish, R. Essick, J. Kanner, E. Katsavounidis, T. B. Littenberg, M. Millhouse, and S. Vitale, "Parameter estimation for gravitational-wave bursts with the bayeswave pipeline", The Astrophysical Journal **839**, 15 (2017).

[48]B. W. Carroll and D. A. Ostlie, *An introduction to modern astrophysics* (Cambridge University Press, 2017).

[49]T. N. P. Organization, *The nobel prize in physics 2017 was divided, one half awarded to rainer weiss, the other half jointly to barry c. barish and kip s. thorne "for decisive contributions to the ligo detector and the observation of gravitational waves."*, `https://www.nobelprize.org/prizes/physics/2017/summary`, 2017.

[50]B. Ryden, *Introduction to cosmology* (Cambridge University Press, 2017).

[51]S. H. Suyu, V Bonvin, F. Courbin, C. D. Fassnacht, C. E. Rusu, D. Sluse, T Treu, K. Wong, M. W. Auger, X Ding, et al., "H0licow–i. h 0 lenses in cosmograil's wellspring: program overview", Monthly Notices of the Royal Astronomical Society **468**, 2590–2604 (2017).

[52]G Dálya, G Galgóczi, L Dobos, Z Frei, I. S. Heng, R Macas, C Messenger, P Raffai, and R. S. de Souza, "GLADE: A galaxy catalogue for multimessenger searches in the advanced gravitational-wave detector era", Monthly Notices of the Royal Astronomical Society **479**, 2374–2381 (2018).

[53]B. P. Abbott et al., "GWTC-1: A Gravitational-Wave Transient Catalog of Compact Binary Mergers Observed by LIGO and Virgo during the First and Second Observing Runs", Physical Review X **9**, 31040 (2019).

[54]B. Abbott, R Abbott, T. Abbott, S Abraham, F Acernese, K Ackley, C Adams, R. Adhikari, V. Adya, C Affeldt, et al., "A gravitational-wave measurement of the hubble constant following the second observing run of advanced ligo and virgo", arXiv preprint arXiv:1908.06060 (2019).

[55]B. Abbott, R Abbott, T. Abbott, S Abraham, F Acernese, K Ackley, C Adams, R. Adhikari, V. Adya, C Affeldt, et al., "Gwtc-1: a gravitational-wave transient catalog of compact binary mergers observed by ligo and virgo during the first and second observing runs", Physical Review X **9**, 031040 (2019).